

Accepted Manuscript

Synthesis and biological evaluation of (1,2,4)triazole[4,3-a]pyridine derivatives as potential therapeutic agents for concanavalin A-induced hepatitis

Yaojie Shi, Qianqian Wang, Juan Rong, Jing Ren, Xuejiao Song, Xiaoli Fan, Mengyi Shen, Yong Xia, Ningyu Wang, Zhihao Liu, Quanfang Hu, Tinghong Ye, Luoting Yu



PII: S0223-5234(19)30550-1

DOI: <https://doi.org/10.1016/j.ejmech.2019.06.025>

Reference: EJMECH 11428

To appear in: *European Journal of Medicinal Chemistry*

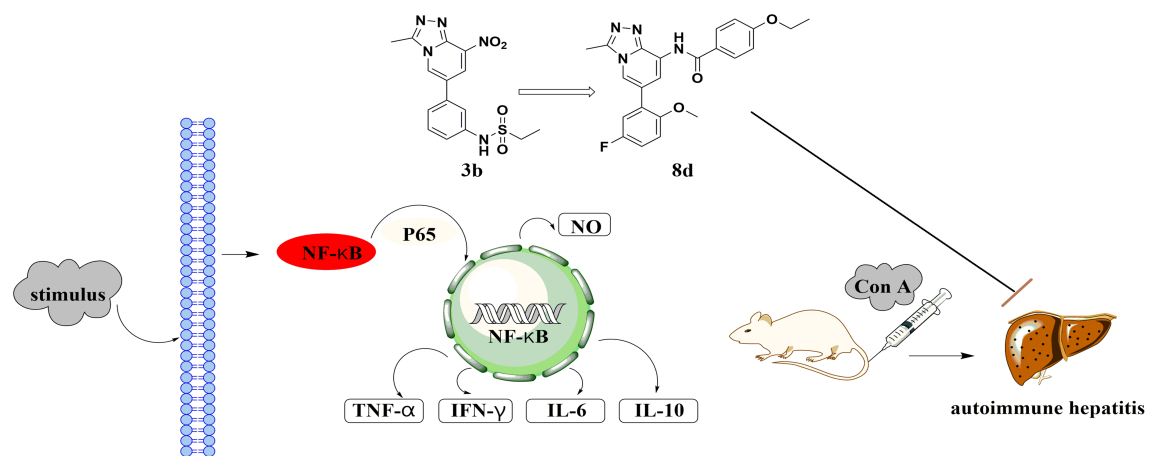
Received Date: 22 April 2019

Revised Date: 28 May 2019

Accepted Date: 8 June 2019

Please cite this article as: Y. Shi, Q. Wang, J. Rong, J. Ren, X. Song, X. Fan, M. Shen, Y. Xia, N. Wang, Z. Liu, Q. Hu, T. Ye, L. Yu, Synthesis and biological evaluation of (1,2,4)triazole[4,3-a]pyridine derivatives as potential therapeutic agents for concanavalin A-induced hepatitis, *European Journal of Medicinal Chemistry* (2019), doi: <https://doi.org/10.1016/j.ejmech.2019.06.025>.

This is a PDF file of an unedited manuscript that has been accepted for publication. As a service to our customers we are providing this early version of the manuscript. The manuscript will undergo copyediting, typesetting, and review of the resulting proof before it is published in its final form. Please note that during the production process errors may be discovered which could affect the content, and all legal disclaimers that apply to the journal pertain.



Synthesis and biological evaluation of (1,2,4)triazole[4,3-a]pyridine derivatives as potential therapeutic agents for concanavalin A-induced hepatitis

Yaojie Shi ^{a,1}, Qianqian Wang ^{a,1}, Juan Rong ^a, Jing Ren ^a, Xuejiao Song ^b, Xiaoli Fan ^c, Mengyi Shen ^c, Yong Xia ^a, Ningyu Wang ^d, Zhihao Liu ^a, Quanfang Hu ^a, Tinghong Ye ^{a,*}, Luoting Yu ^{a,*}

^a Laboratory of Liver Surgery, State Key Laboratory of Biotherapy and Cancer Center, West China Hospital, Sichuan University and Collaborative Innovation Center of Biotherapy, Chengdu, Sichuan, 610041, China.

^b Research Center for Public Health & Preventive Medicine, West China School of Public Health & Healthy Food Evaluation Research Center/No.4 West China Teaching Hospital, Sichuan University, Chengdu, Sichuan, 610041, China.

^c Division of Digestive Diseases, West China Hospital, West China Medical School, Sichuan University, Chengdu, 610041, China.

^d School of Life Science and Engineering, Southwest JiaoTong University, Chengdu, Sichuan, 611756, China.

* Corresponding author. State Key Laboratory of Biotherapy, West China Hospital, Sichuan University and Collaborative Innovation Center of Biotherapy, Chengdu, Sichuan, 610041, China. E-mail: yeth1309@scu.edu.cn; yuluot@scu.edu.cn; Fax: +86 28 8516 4060; Tel: +86 28 8516 4063.

¹ These authors contribute equally to this work.

Highlights

A series of new (1,2,4)triazole[4,3-a]pyridine derivatives were synthesized.

8d suppressed NF- κ B p65 translocation and expression of inflammatory genes.

Preliminary mechanisms of anti-inflammatory action were discovered.

8d could be a lead compound as AIH therapeutic agent.

Abstract

A series of (1,2,4)triazole[4,3-a]pyridine (TZP) derivatives have been designed and synthesized. Compound **8d** was identified as having the most potent inhibitory activity on NO release in response to lipopolysaccharide (LPS) stimulation and inhibition of the migration induced by MCP-1 protein on RAW264.7 macrophages. Based on the screening data, an immunofluorescence assay and a real-time qPCR assay were conducted, indicating that compound **8d** suppressed NF- κ B p65 translocation and expression of inflammatory genes by concanavalin A (Con A)-induced RAW264.7 macrophages. More importantly, **8d** also exhibited potent efficacy, alleviating Con A-induced hepatitis by downregulating the levels of plasma alanine transaminase (ALT), aspartate transaminase (AST) and inflammatory infiltration in a mouse autoimmune hepatitis (AIH) model. In addition, the flow cytometry (FCM) data showed that compound **8d** inhibited the accumulation of MDSCs in the liver of Con A-induced mice. These findings raise the possibility that compound **8d** might serve as a potential agent for the treatment of AIH.

Keywords: triazole[4,3-a]pyridine anti-inflammatory AIH

1. Introduction

Inflammation is part of the complex biological response of body tissues to infection and injury and is a protective response involving the recruitment of immune systems and molecular mediators to eliminate the initial cause of cell injury¹. Prolonged activation of the immune system is associated with activation of inducible NO synthase (iNOS) and the release of pro-inflammatory cytokines, such as nitric oxide (NO) and tumor necrosis factor-alpha (TNF- α), which play an important role in inflammation cascades. The excessive inflammatory activation or deregulation of mechanisms of the subsequent removal of inflammatory cells from the inflammatory microenvironment may underlie a vast variety of diseases, including autoinflammatory diseases, inflammatory bowel disease^{2,3}, rheumatoid arthritis and autoimmune hepatitis (AIH)⁴.

AIH is a chronic autoimmune liver disease with an unknown pathogenesis where the body's immune system attacks liver cells, causing the liver to be inflamed. It was first described by Jan Waldenström and Henry Kunkel independently in the early 1950s⁵. Although AIH by definition is a chronic disease that may lead to cirrhosis, hepatocellular carcinoma (HCC), and/or death, it is characterized by elevated transaminase levels and a mixed histological infiltrate of plasma cells and lymphocytes. Sustained immunosuppressive therapy with a high dose of prednisolone with or without azathioprine is the standard therapy⁶ for alleviating liver inflammation and fibrosis and to induce remission (a decrease in serum aminotransferase) and prevent liver decompensation⁴.

Long-term treatment with prednisolone may cause cosmetic changes such as weight gain, acne, moon face, and severe side effects including osteopenia and malignancy^{7, 8}. The most common side effects of azathioprine are cytopenia, nausea, arthralgia, fever, and skin rash, and some patients may even develop severe side effects such as cholestatic hepatitis, pancreatitis, opportunistic infections and bone marrow suppression^{7, 8}. Although some patients remain in remission after drug treatment is withdrawn, most require long-term maintenance therapy. Additionally, many patients are not responsive to standard treatment or fail to achieve a remission, and therefore, there is an urgent need for novel and perhaps a small molecules-based approach to AIH. Con A-induced model is a typical animal model for investigating T-cell and macrophage dependent hepatitis in mice, which closely mimics the pathogenesis mechanisms and pathological changes of patients, and provides a valuable tool for rapidly assessing novel therapeutic approaches for AIH⁹.

NO is a gaseous signaling molecule that plays an important role in various physiological processes¹⁰ especially in inflammation^{11, 12}. Since the identification of NO as an endothelium-derived endogenous messenger responsible for vascular smooth muscle relaxation^{13, 14}, there has been a burst of research into this key messenger. A large body of evidence supports the direct role of NO in inflammation¹⁵ and tissue injury. In addition, the number of researchers who have delved into understanding how NO regulates tumor immunology¹⁶, allergy and autoimmunity¹⁷ has increased in the past decade. NO modulates transcription/translation indirectly by affecting signaling pathways, such as mitogen activated protein kinase, phosphatidylinositol-3 kinase, G-protein¹⁸ and NF-kappa B¹⁹.

Overproduction of NO by iNOS generally destroys functional normal tissues during inflammation. Alterations in NO synthesis by endogenous systems can influence these inflammatory processes²⁰ and macrophages are the most representative iNOS-expressing innate immune cells²¹. These findings suggest that evaluating the NO releasing level may be a promising method for screening of anti-inflammation agent/compounds. In our continued concern about new potential small molecules that can be used as anti-inflammation agents, screening of our small molecule library was carried out, leading to the discovery of compound **3b** (**Figure 1**), which is a triazolopyridine derivative. The triazolopyridines have been identified as one of the promising scaffolds in medicinal chemistry, which possess a wide range of biological activities, such as p38 inhibitors²²⁻²⁵, c-Met inhibitors²⁶, protein tyrosine kinase modulators²⁷ and dipeptidyl peptidase IV inhibitors²⁸.

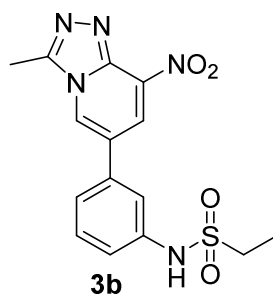
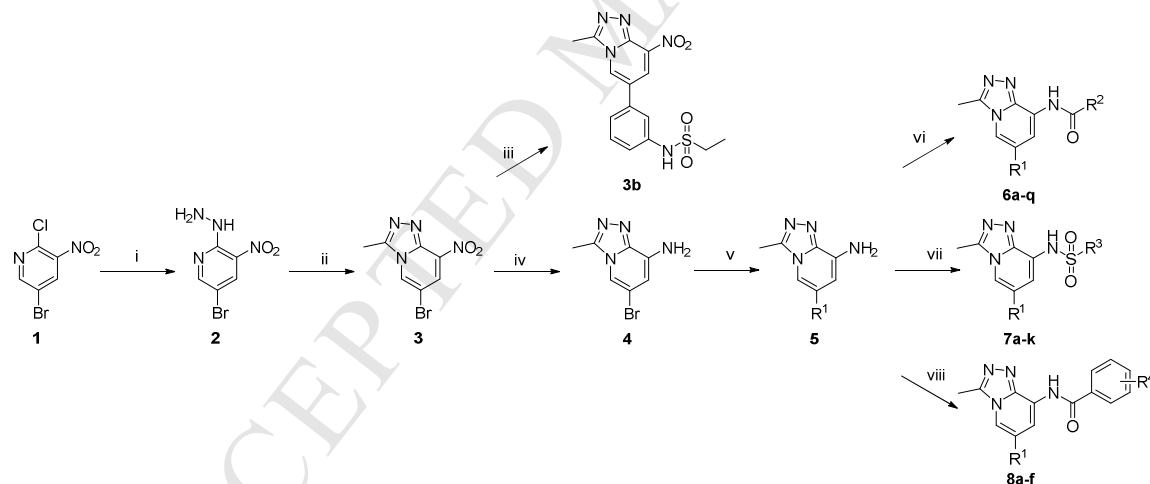


Figure 1. Structure of Compound 3b.

We focused our attention on the (1,2,4)triazolo[4,3-a]pyridine (TZP) motif owing to the (1,2,4)triazole core structure being able to serve as a suitable hydrogen bonding acceptor, which is thought to be essential for its pharmacological activity. In the current study, we designed and prepared the derivatives of TZP depicted in Scheme 1. Considering the potential toxicity of nitro compounds, we reduced the nitro group at the 8-position of TZP for substitution with different materials. Structure-activity relationship (SAR) optimization of substituents at the C-6 and C-8 positions of the TZP core resulted in the identification of compound 8d as a potent inhibitor of NO release evoked by LPS and the expression of TNF- α , IFN- γ , IL-6 and IL-10 cytokine mRNAs induced by Con A in RAW264.7 macrophages.



Scheme 1. Synthesis of TZP Derivatives.

Reagents and conditions: (i) $N_2H_4 \cdot H_2O$, 1,4-dioxane, reflux, 1 h; (ii) trimethyl orthoacetate, 1,4-dioxane, reflux, 1 h; (iii) substituted boric acid, $Pd(dppf)_2Cl_2$, Na_2CO_3 , 1,4-dioxane/ H_2O , 90 °C, 4–6 h; (iv) Fe, NH_4Cl , THF/ $EtOH/H_2O$, 90 °C, 1 h; (v) substituted boric acid or borate, $Pd(dppf)_2Cl_2$, Na_2CO_3 , 1,4-dioxane/ H_2O , 90 °C, 4–6 h; (vi) acetyl chloride or cyclohexane carboxylic acid chloride or cyclobutane carboxylic acid chloride, K_2CO_3 , DCM, 0 °C-rt; (vii) ethanesulfonyl chloride, Et_3N or pyridine, DCM, 0 °C-rt; and (viii) aromatic acid chloride, pyridine, DCM, 0 °C-rt.

2. Results and discussion

2.1 Chemistry

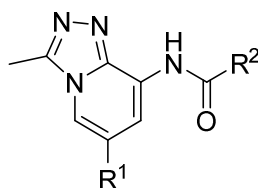
The synthesis of TZP derivatives is depicted in **Scheme 1**. The key intermediate 6-bromo-3-methyl-[1,2,4]triazolo[4,3-a]pyridin-8-amine (**4**) for the preparation was synthesized from 5-bromo-2-chloro-3-nitropyridine that was treated with hydrazine hydrate in 1,4-dioxane. Then, the crude product **2** was heated to reflux in the presence of trimethyl orthoacetate to produce compound **3**, which was directly reduced by Fe/NH₄Cl to the target compound **4**. Subsequently, substituted boric acid or borate with bromopyridine **4** under standard Suzuki-Miyaura coupling conditions provided intermediate **5** in good yield. Amidation or sulfonylation gave target compounds **6a–q**, **7a–k**, and **8a–f** in excellent yield. The characterization of individual target compounds can be found in the Supporting Information. Individual compounds with a purity of >95% were used for the subsequent experiments.

2.2 Biology evaluation

2.2.1 Measurement of NO production in murine RAW264.7 macrophages upon LPS stimulation

Macrophages are important effector cells in the inflammatory response process and respond to pathogenic agents by synthesizing NO from iNOS. The NO production inhibitory activities of the TZP derivatives at a concentration of 20 μM were measured in RAW264.7 macrophages after lipopolysaccharide (LPS) treatment. The ability (relative amount of NO compared to LPS %) of the tested compounds to reduce NO release is summarized in Tables 1–3 and Figure 2. As shown in Table 1 and Figure 1, NO production in LPS-stimulated RAW264.7 macrophages was suppressed by compounds **6a–q** after 24 h incubation. Among them, when R² is methyl, **6j** with 2,5-disubstituted in the R¹ benzene ring, exhibited remarkable inhibitory activity against LPS-induced RAW264.7 macrophages NO production with an relative amount of 27.05±0.34%. The above results indicated that the introduction of 5-chloro in R¹ increased its activity. In addition, replacement of the 2-benzyloxy in R¹ (**6j**) with 2-alkoxy, including methoxy (**6k**), ethoxy (**6l**), and propoxy (**6m**), slightly decreased the inhibitory activity. However, **6m** shows a comparable activity with **6j**. Thus, we can make a statement that phenoxy and alkoxy are needed for the inhibitory activity of the TZP derivatives of compounds **6a–q**. With the introduction of cyclohexyl in R², compounds **6p–q** showed less potency than **3b**. In addition, comparing the activities of compound **6o** with 2-methoxypyridine in R¹ and **6a–g**, the results shown in Table 1 indicate that the aromatic heterocyclic ring in R¹ is compatible with the activity.

Table 1. NO release relative amount of compounds **6a–q**

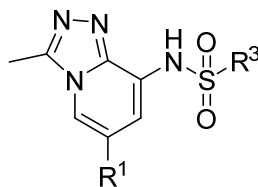


Compound	R ¹	R ²	relative amount of NO compared to LPS %
6a	Ph	Me	44.71±1.19
6b	<i>o</i> -Cl-phenyl	Me	48.41±1.04
6c	<i>o</i> -F-phenyl	Me	83.06±6.16
6d	<i>o</i> -CF ₃ -phenyl	Me	42.36±0.59
6e	<i>m</i> -OMe-phenyl	Me	55.30±0.34
6f	<i>m</i> -NHSO ₂ Et-phenyl	Me	64.96±4.09
6g	<i>m</i> -OCF ₃ -phenyl	Me	49.52±3.52
6h	4-morpholinomethyl-phenyl	Me	42.40±0.01
6i	1,1'-biphenyl-2-yl	Me	49.03±1.12
6j	2-benzyloxy-5-Cl-phenyl	Me	27.05±0.34
6k	2-OMe-5-Me-phenyl	Me	58.83±3.15
6l	2-OEt-5-Me-phenyl	Me	32.07±2.49
6m	5-Cl-2-propoxy-phenyl	Me	49.05±2.37
6n	2-OEt-4-F-phenyl	Me	65.85±3.74
6o	2-methoxypyridine	Me	54.04±3.91
6p	2-OEt-5-F-phenyl	cyclohexyl	37.80±1.44
6q	2-methoxypyridine	cyclohexyl	49.99±1.61
3b	-	-	26.74±0.57
LPS	-	-	96.06±1.40

In consideration that sulfonamide is an important pharmacophore having attractive pharmacological properties, compounds **7a–k** were rapidly synthesized by using ethanesulfonyl chloride reacting with intermediate **5**. As shown in Table 2, most of the synthesized TZP analogues showed inhibitory potency except **7e**. Among them, **7b** and **7j** showed significant inhibitory activities of NO production, especially **7j** that showed better activity than **3b**. Compared with **6j** and **7j**, this further indicated that 2,5-disubstituted in the R¹ benzene ring is important for the activity. However, when compared with the activities of bulky group-substituted derivatives, including compounds **7f**, and **7g**, the results suggested that a bulky group is not an optimal group

for the development of an inhibitory activity on NO release. Similarly, comparing compounds **6o** and **7a–d**, the results indicated that an aromatic heterocyclic ring in R¹ is compatible with the activity.

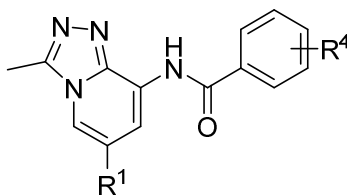
Table 2. NO release relative amount of compounds **7a–k**



Compound	R ¹	R ³	relative amount of NO compared to LPS %
7a	Ph	Et	44.44±0.71
7b	<i>m</i> -CF ₃ -phenyl	Et	27.18±1.22
7c	<i>m</i> -NHSO ₂ Et-phenyl	Et	41.19±1.23
7d	<i>o</i> -CF ₃ -phenyl	Et	58.67±2.88
7e	<i>o</i> -Cl-phenyl	Et	152.42±4.59
7f	1,1'-biphenyl-2-yl	Et	62.68±1.13
7g	2-benzyloxy-phenyl	Et	72.57±6.33
7h	2-OMe-5-Me-phenyl	Et	45.48±3.49
7i	2-OEt-4-F-phenyl	Et	34.85±0.83
7j	2-benzyloxy-5-Cl-phenyl	Et	26.01±0.62
7k	2-methoxypyridine	Et	49.93±0.86
3b	-	-	26.74±0.57
LPS	-	-	102.81±1.90

On the basis of the above results, eight TZP analogues **8a–f** were synthesized by replacing the R² by benzene rings with different substitutions. Consistent with the above SAR analysis, 2,5-substituted in R¹ is the optimal group for the activity as shown in Table 3 (**8d–f**). Among them, compound **8d** with a 5-F-2-OMe-phenyl group at the R¹-moiety and *p*-OEt group at the R⁴-moiety exhibited better activity than **3b** with relative amount of 28.01±0.29%. It is also worth mentioning that *p*-substituted in R⁴ is advantageous for the inhibitory activity, such as **8d** with *p*-OEt substituted. In contrast, *o*-substituted in R⁴ is disadvantageous for the inhibitory activity, such as **8c** with *o*-F substituted.

Table 3. NO release relative amount of compounds **8a–f**



Compound	R ₁	R ₄	relative amount of NO compared to LPS %
8a	<i>p</i> -Cl-phenyl	<i>p</i> -F	42.88±0.58
8b	<i>p</i> -Cl-phenyl	<i>m</i> -CF ₃	30.98±2.39
8c	5-Cl-2-propoxy-phenyl	<i>o</i> -F	77.73±1.20
8d	5-F-2-OMe-phenyl	<i>p</i> -OEt	28.01±0.29
8e	5-F-2-OMe-phenyl	2,6-diF	61.96±2.76
8f	5-F-2-OMe-phenyl	4-benzyloxy-2-Cl	32.06±1.37
3b	-	-	26.74±0.57
LPS	-	-	99.19±2.17

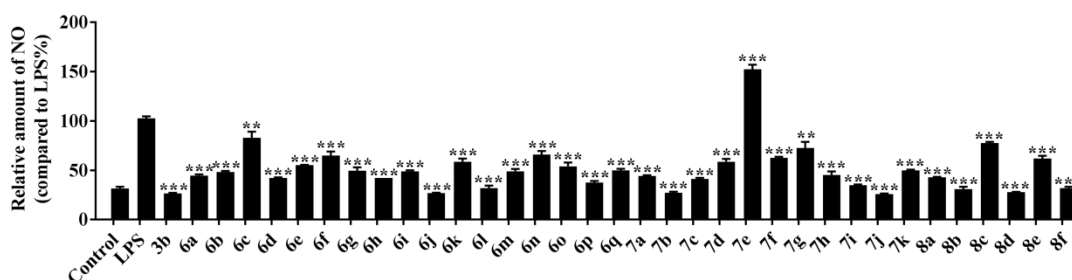


Figure 2. Inhibition of NO release by compounds 6a–q, 7a–k and 8a–f

RAW264.7 cells were pretreated with compounds **6a–q** for 1 h, incubated with LPS (1 μ g/mL) for another 23 h, NO release was measured using Griess Reagent assay (***) $p < 0.001$, ** $p < 0.01$).

2.2.2 Measurement of inhibition of the migration of RAW264.7 macrophages induced by MCP-1 protein

Macrophage migration ability plays an essential role and is a prerequisite for their participation in immune and inflammatory responses²⁹. Monocyte chemoattractant protein-1 (MCP-1), also known as chemokine (C-C motif) ligand 2 (CCL2), appears to be an important component of the recruitment of macrophages to inflammatory lesions³⁰. Deregulated migration of macrophages has been implicated in a variety of human disorders, such as chronic inflammation, neurodegenerative disease and tumor metastasis²⁹. To evaluate the inhibitory effects of TZP derivatives on

MCP-1-mediated chemotactic responses, we conducted chemotactic migration assays to investigate the effects of synthetic compounds on the migration of RAW264.7 cells. Given the structures of the different series, we chose representative compounds that had striking inhibitory activities on NO release relative amount, shown in Figure 3. AS605240³¹, an established PI3K γ inhibitor, was used as the reference agent and has been proven to ameliorate Con A-induced liver injury in a murine model³².

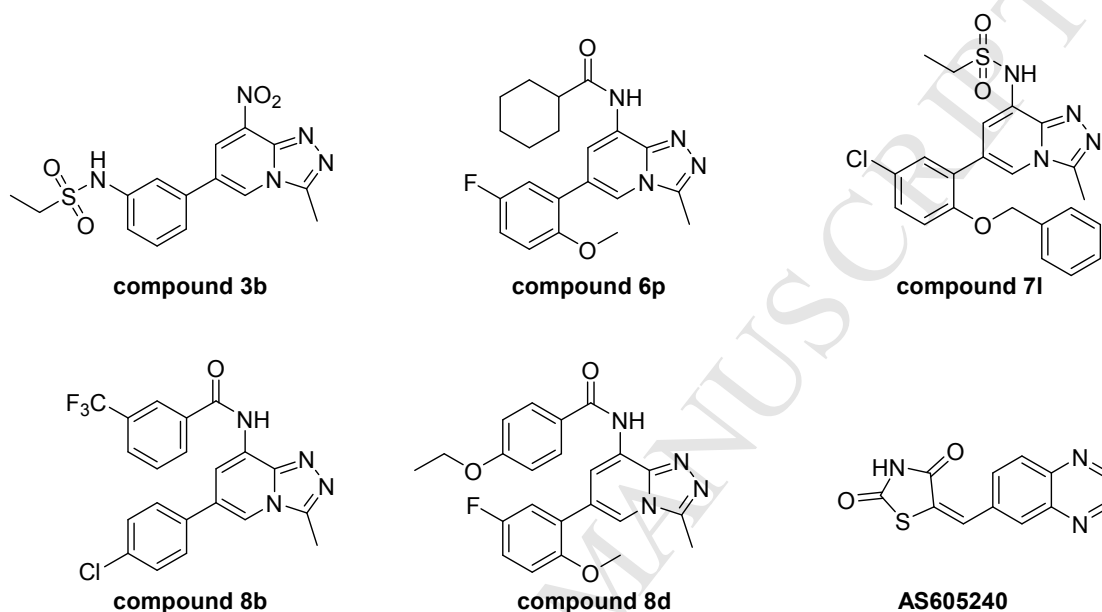


Figure 3. Structures of representative TZP derivatives and AS605240.

As illustrated in Figure 4, the tested compounds showed different inhibitory effects on cell migration at a concentration of 20 μ M. Interestingly, compound **6p**, that only showed a mild NO release inhibitory activity, has an excellent inhibitory rate against MCP-1 mediated chemotaxis. In contrast to that, compound **7l**, which **showed** an outstanding NO release inhibitory activity, had a much lower activity on RAW264.7 macrophages chemotaxis.

Among these derivatives, compound **8d** showed the most potent and better activity than that of AS605240, with inhibitory rate of $52.59 \pm 7.39\%$ and 40.55 ± 6.05 ($P < 0.001$), respectively. Compound **8d** also exhibited an effective inhibition activity on the LPS stimulated RAW264.7 macrophages NO release inhibitory activity. Due to these results, **8d** is quite worthy of undergoing further biological assays to identify if it could be a potential agent for AIH treatment.

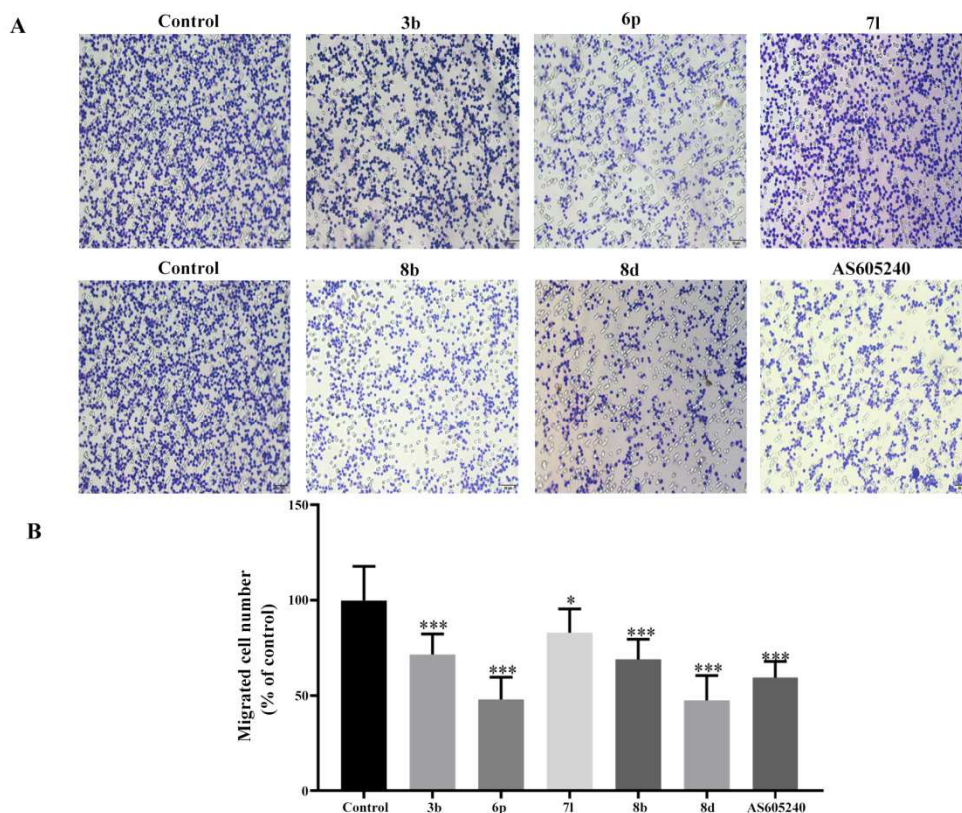


Figure 4. Inhibitory effect of compounds on migration of RAW264.7 macrophages induced by MCP-1. The migration of RAW264.7 cells were analyzed using a chemotactic migration assay. A. Cells were photographed after compounds (20 μ M) treatment for 3 h (n=3). B. The quantification results for the chemotactic migration assay. Five different areas of migrated cells were counted for each well (n = 3; * P<0.05 versus control group, *** P<0.001 versus control group).

2.2.3 Compound 8d suppresses NF- κ B p65 translocation

Transcription factor NF- κ B signaling is pivotal in the induction of inflammatory responses and the production of inflammatory cytokines³³. When NF- κ B activation is induced by stimulus (Con A or LPS), I κ B is phosphorylated and degraded, which leads to the release of the NF- κ B p65 subunit from the cytoplasm, followed by translocation to the nucleus, where it binds to target promoters and turns on the transcription of inflammatory genes including TNF- α and IL-6.

Herein, the effect of compound **8d** on NF- κ B p65 subunit nuclear translocation was determined by an immunofluorescence assay. As shown in Figure 5, the NF- κ B subunit p65 was almost exclusively observed in the cytoplasm in the un-stimulated RAW264.7 macrophages. After stimulation with Con A (0.6 μ M) or LPS (1 μ g/mL) for 2 h, most cytoplasmic p65 translocated into the nucleus (green dots in the blue nucleus). In compound **8d** (concentration were indicated

on Figure 5 A and C) treated cells, nuclear localization of p65 was significantly reduced on a dose-dependent manner, suggesting that compound **8d** inhibited p65 translocation from the cytoplasm to nuclei. In all, these results suggest that the anti-inflammatory activity of compound **8d** may be closely associated with its inhibitory effects on NF- κ B pathways.

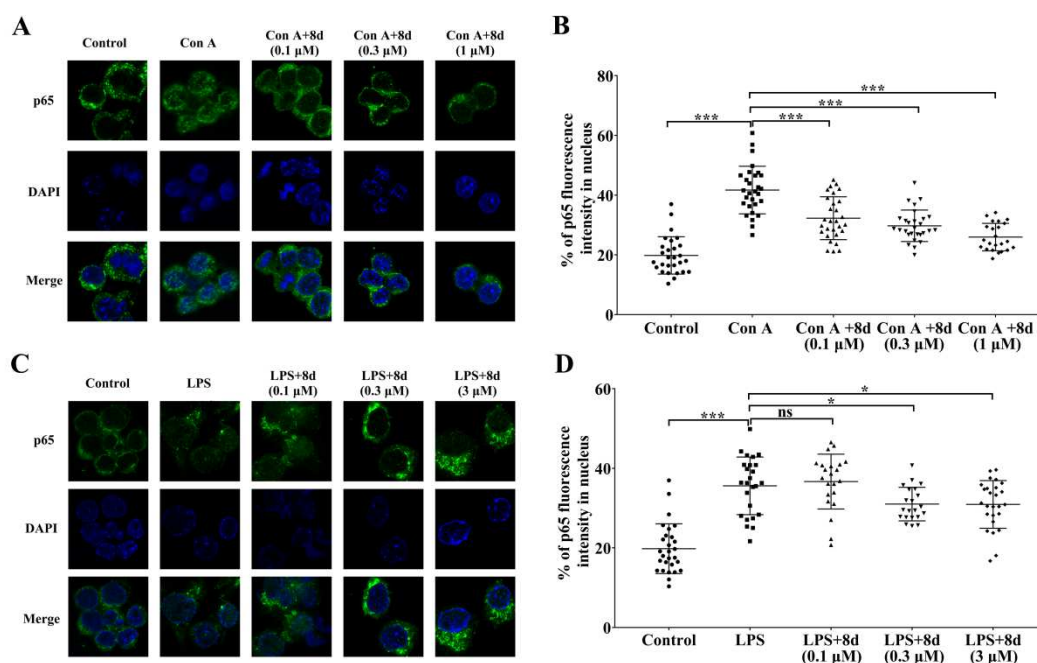


Figure 5. Compound 8d exhibited potent inhibitory effects on nuclear translocation of p65 in Con A-stimulated RAW264.7 macrophages. Cells were treated with Con A for 2 h followed by compound **8d** (1 μ M) for another 22 h. The subcellular localization of p65 was determined by immunofluorescence. A. C. Photographs were taken using a laser-scanning confocal microscope. B. D. The quantification of nuclear translocation of p65 (≥ 5 foci) presented in each group was compared (** $P < 0.01$).

2.2.4 Effect of compound 8d on the expression of inflammatory genes in Con A-induced RAW264.7 macrophages

The inflammatory signaling of Con A-induction results in the production of a variety of cytokines, chemokines, and inflammation mediators. To evaluate whether the inhibitory effect on inflammatory response caused by compound **8d** occurs at the transcriptional level, the mRNA expression of inflammatory genes (various cytokines) such as IFN- γ , IL-6, IL-10 and TNF- α in RAW264.7 macrophages were measured with real-time quantitative PCR. As shown in Figure 6, upregulated cytokine gene expression triggered by Con A was blocked by compound **8d**. Furthermore, the mRNA expression levels in macrophages of TNF- α , IFN- γ , IL-6, and IL-10 were decreased by compound **8d** at 1 μ M.

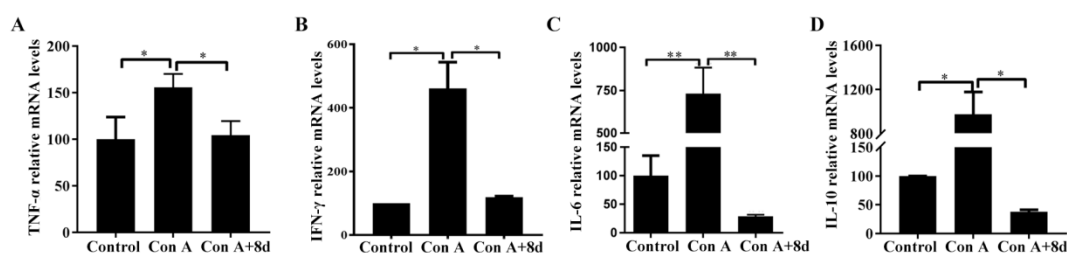


Figure 6. Compound 8d regulates mRNA expression of various cytokines, including TNF- α , IFN- γ , IL-6 and IL-10. RAW 264.7 macrophages were pretreated with Con A for 2 h followed by compound **8d** (1 μ M) for another 22 h. The results are normalized to the reference gene GAPDH, and the values shown are mean \pm SD (n=5, *p < 0.05; **p < 0.01).

2.2.5 Cytotoxicity Assay

The cytotoxicity of all synthesized compounds was evaluated in LO₂ cells by MTT assay after 24 h of treatment. As observed from Figure 7, all compounds (20 μ M) showed no obvious cytotoxicity on LO₂ cells.

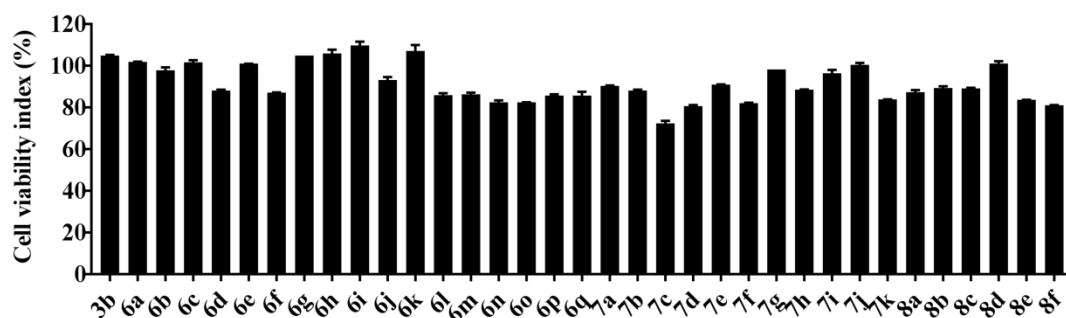


Figure 7. Effect of compounds on the viability of the human normal liver cell line LO₂. The effect of all synthesized compounds on cell viability was estimated by MTT assay.

2.2.6 Effect of compound 8d on a Con A-induced AIH mouse model *in vivo*

The anti-inflammatory activity of compound **8d** was determined in a Con A-induced AIH mouse model^{9,34}. As shown in Figure 8, compared with the normal control mice, the mice injected with Con A (20 mg/kg) developed AIH as characterized by elevated levels of serum alanine transaminase (ALT) and aspartate transaminase (AST). After intraperitoneal administration of compound **8d** (100 mg/kg), the serum levels of ALT and AST were significantly decreased at 12 h after Con A injection. Compound **8d** significantly reduced the activity levels of ALT and AST by **65.39%** and **52.52%**, respectively, compared with the model group (p < 0.01). The results indicated that treatment with compound **8d** ameliorated the severity of AIH caused by Con A.

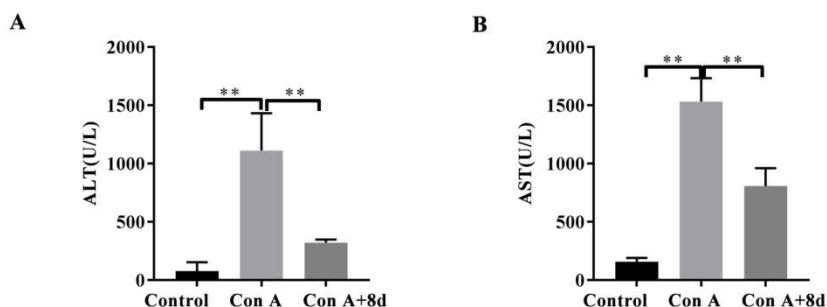


Figure 8. The levels of liver transaminase after Con A administration. Alanine aminotransferase (ALT), aspartate transaminase (AST). Values are mean \pm SD. (n=5, ** p < 0.01).

2.2.7 Histological Examination of the Liver

Histological features have prominent roles in the diagnosis and treatment of AIH^{35, 36}. Thus, a liver biopsy and HE staining assay is necessary for investigating whether compound **8d** impaired recruitment of macrophages to the liver tissue. As shown in Figure 9, dramatic inflammatory cell infiltration around the central vein areas, massive hepatocytes necrosis, and disordered hepatic sinusoid structures were observed in Con A-treated mice. Furthermore, administration of compound **8d** decreased the necrosis of hepatocytes. The effects of compound **8d** on the infiltration of CD4⁺ T cells, F4/80⁺ macrophages and CD11b⁺ cells in the livers were determined. Figure 8 shows that the numbers of CD4⁺ T cells, F4/80⁺ macrophages and CD11b⁺ cells increased significantly in the livers after Con A injection, but could be returned to basal levels by compound **8d** treatment. We inferred from these results that **8d** had significant hepatoprotective effects in the Con A-induced AIH model.

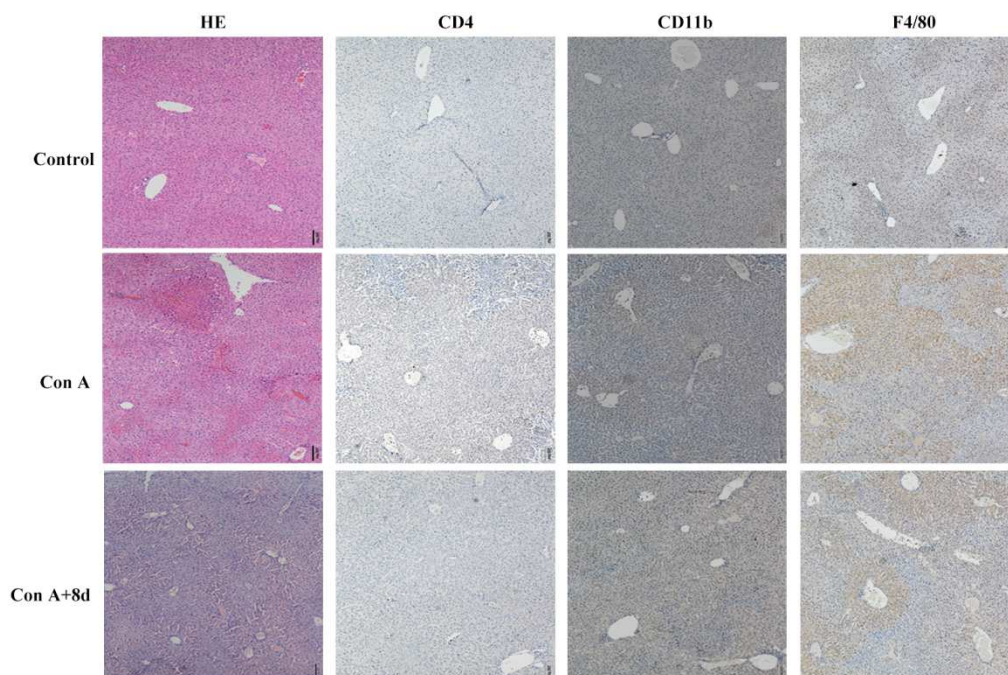


Figure 9. Hematoxylin and eosin (H&E) staining and expression profiling of CD4⁺, F4/80⁺ and CD11b⁺ cells in livers.

2.2.8 The influence of compound 8d on the MDSCs population frequency/flow cytometry

Myeloid-derived suppressor cells (MDSCs) play a key role in immune responses during AIH. Therefore, we assessed the MDSCs in the liver after Con A treatment with or without compound **8d**. We used the Gr-1 and CD11b antibodies to identify MDSCs. As illustrated in Figure 10 A, after intravenous injection (i.v.) of Con A, there was a significant accumulation of myeloid-derived suppressor cells (MDSCs) in the liver in Con A treatment mice compared to normal control mice (Figure 10 A). In more detail, MDSCs in the saline group were 4.46% while MDSCs in the Con A group reached 11.31%, and the difference was statistically significant ($p < 0.05$).

Moreover, further analysis indicated that the administration of compound **8d** at 100 mg/kg decreased the percentage of MDSCs to 8.39% (Figure 10 B) and thus inhibited the accumulation of MDSCs in the liver.

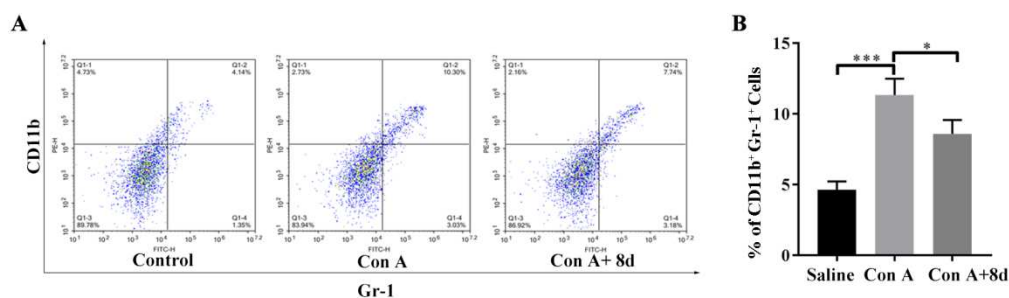


Figure 10. Compound 8d inhibited the accumulation of macrophages in the liver of mice stimulated by Con A. Bars show the mean \pm SD (n=5, * p < 0.05, *** p < 0.001).

3. Conclusion

In summary, with the aim of finding compounds with efficient anti-inflammatory activity, forty-one TZP derivatives were synthesized. The results of the initial evaluation showed that some compounds exhibited effective NO release inhibitory activity. Among them, 4-ethoxy-N-(6-(5-fluoro-2-methoxyphenyl)-3-methyl-[1,2,4]triazolo[4,3-a]pyridin-8-yl)benzamide (compound **8d**) showed the most potent inhibitory activity on the migration of RAW264.7 macrophages and the NO release inhibitory activity. The preliminary mechanism of its anti-inflammatory action indicated that the compound could significantly suppress the expression of TNF- α , IFN- γ , IL-6 and IL-10 and the production of NO through affecting the NF- κ B signaling pathway. In addition, compound **8d** ameliorated the severity of AIH in a Con A-induced mouse model.

4. Experimental section

4.1 Chemistry

4.1.1. General

Chemical reagents of analytical grade were purchased from Shanghai Bidepharmatech Ltd., Shanghai, PRC. The reactions were monitored by thin layer chromatography (TLC) on precoated silica GF254 plates under UV light at 254 and 365 nm. ^1H NMR spectra were recorded on a Bruker AM-400 AVANCE^{III} (400 MHz) spectrometer with CDCl_3 and $\text{DMSO}-d_6$ as the solvent. MS spectra were recorded on a Waters Q-TOF (ESI). Individual compounds with a purity of >95% (Dionex UltiMate 3000) were used for subsequent experiments.

4.1.2. General Procedure for the Synthesis of Intermediate 4

To a suspension of 5-bromo-2-chloro-3-nitropyridine (compound **1**, 42 mmol) in 1,4-dioxane (50 mL) at room temperature was added hydrazine hydrate (98% in water) (84 mmol). The reaction mixture was stirred at 110 °C for 1 h. Upon completion (judged by TLC), the reaction mixture was allowed to cool at room temperature and the solvent was evaporated. After that, water (100 mL) was added and the reaction mixture was extracted with ethyl acetate (100 mL \times 3). The combined organic phase was washed with brine (100 mL), dried over sodium sulfate and evaporated under reduced pressure. The crude product was used for the next step without further purification³⁷.

To a solution of compound **2** (10 mmol) in 1,4-dioxane (50 mL) was added trimethyl orthoacetate (100 mmol) at room temperature. The reaction mixture was heated to reflux for about 1 hour, at which time TLC indicated near complete consumption of the starting material compound **2**. The solvent was removed by rotary evaporation. The residue was diluted with DCM and water. The aqueous layer was extracted twice with DCM. The combined organic layers were dried over Na₂SO₄ and concentrated by rotary evaporation. The crude mixture was subjected to column chromatography (PE:EtOAc = 6:1~1:1) to afford the product compound **3** as a yellow solid (82% yield, two steps)³⁸.

To a solution of compound **3** (5 mmol) in EtOH (5 mL) and THF (5 mL) containing ammonium chloride (10 mmol) and H₂O (2 mL) was added Fe powder (10 mmol) in portion with rapid stirring at 50 °C. The temperature of the reaction was then raised to 100 °C. After 1 hour, the reaction was filtered, and the residual iron was washed with EtOAc. The organic layers were then washed with water and brine, dried over Na₂SO₄, and concentrated in vacuo to provide the aniline product compound **4** (86% yield) that was sufficiently pure to carry on to the next step³⁹.

4.1.3. General Procedure for the Preparation of **3b**

A mixture of compound **3** (4 mmol), (3-(ethylsulfonamido)phenyl)boronic acid (4.8 mmol), [1,1'-Bis(diphenylphosphino)ferrocene]dichloropalladium(II) (5 mol %), and sodium carbonate (12 mmol) in 1,4-dioxane (10 mL) and water (5 mL) was heated under nitrogen conditions (90 °C, 6 h). After cooling to ambient temperature, the reaction mixture was filtered and concentrated. The residue was partitioned between water and dichloromethane. The organic layer was separated and purified by flash chromatography to get compound **3b** (78%).

3b: Light yellow powder, 78% yield. ¹H NMR (400 MHz, Chloroform-*d*, δ ppm) 9.01 (d, *J* = 1.7 Hz, 1H), 8.72 (d, *J* = 1.7 Hz, 1H), 7.57 – 7.50 (m, 2H), 7.44 – 7.39 (m, 1H), 7.35 – 7.30 (m, 1H), 6.94 (s, 1H), 3.22 (q, *J* = 7.4 Hz, 2H), 2.74 (s, 3H), 1.43 (t, *J* = 7.4 Hz, 3H). ESI-HRMS *m/z*: 362.0923, [M+1]⁺, calcd for C₁₅H₁₅N₅O₄S: 361.0845.

4.1.4. General Procedure for the Preparation of **6a–q**

A mixture of compound **4** (2 mmol), boric acids or borates (2.4 mmol), [1,1'-bis(diphenylphosphino)ferrocene]dichloropalladium(II) (**5 mol %**), and sodium carbonate (6 mmol) in 1,4-dioxane (8 mL) and water (4 mL) was heated under nitrogen conditions (90 °C, 6 h). After cooling to ambient temperature, the reaction mixture was filtered and concentrated. The residue was partitioned between water and dichloromethane. The aqueous layer was extracted with dichloromethane three additional times. The combined organic layers were washed with saturated

aqueous sodium chloride, dried over anhydrous sodium sulfate, filtered, and concentrated. The residue was purified by flash chromatography to provide compounds **5a–q**.

We added acetyl chloride or cyclohexanecarboxylic acid chloride or cyclobutanecarbonyl chloride (1.5 mmol) dropwise to a solution of each individual compound **5a–q** (1 mmol), anhydrous dichloromethane (5 mL) and potassium carbonate (1.5 mmol) at 0 °C under stirring. The mixture was stirred at room temperature for 1 h until TLC showed the reaction was complete. The reaction mixture was diluted with dichloromethane and washed with water. The organic extract was dried, concentrated and purified by column chromatography using silica gel to produce the compounds **6a–t** as off white solids⁴⁰.

6a: White powder, 87% yield. ¹H NMR (400 MHz, Chloroform-*d*, δ ppm) 8.74 (d, $J = 1.6$ Hz, 1H), 8.39 (d, $J = 1.6$ Hz, 1H), 8.32 (s, 1H), 7.64 – 7.57 (m, 2H), 7.48 (t, $J = 7.4$ Hz, 2H), 7.44 – 7.39 (m, 1H), 2.62 (s, 3H), 2.32 (s, 3H).

¹³C NMR (101 MHz, Chloroform-*d*, δ ppm) 170.19, 162.43, 160.10, 143.68, 137.79, 130.18, 129.02, 126.00, 119.76, 119.59, 116.95, 24.14, 14.21. ESI-HRMS m/z : 267.1246, $[M+1]^+$, calcd for C₁₅H₁₄N₄O: 266.1168.

6b: Off-white powder, 69% yield. ¹H NMR (400 MHz, Chloroform-*d*, δ ppm) 8.57 (s, 1H), 8.56 (d, $J = 1.5$ Hz, 1H), 8.29 (d, $J = 1.5$ Hz, 1H), 7.50 (m, 1H), 7.38 (m, 3H), 2.61 (s, 3H), 2.30 (s, 3H).

¹³C NMR (101 MHz, Chloroform-*d*, δ ppm) 169.26, 162.92, 143.94, 135.68, 133.04, 131.51, 130.23, 129.71, 127.16, 126.38, 125.53, 122.08, 117.97, 24.61, 14.30. ESI-HRMS m/z : 301.0864, $[M+1]^+$, calcd for C₁₅H₁₃ClN₄O: 300.0778.

6c: Off-white powder, 76% yield. ¹H NMR (400 MHz, Chloroform-*d*, δ ppm) 8.67 (s, 1H), 8.45 (s, 1H), 8.44 (t, $J = 1.4$ Hz, 1H), 7.51 (m, 1H), 7.39 (m, 1H), 7.27 (m, 1H), 7.19 (m, 1H), 2.62 (s, 3H), 2.31 (s, 3H).

¹³C NMR (101 MHz, Chloroform-*d*, δ ppm) 169.24, 162.99, 159.74 (d, $J = 249.8$ Hz), 143.96, 130.65 (d, $J = 2.9$ Hz), 130.10 (d, $J = 8.3$ Hz), 125.92, 124.77 (d, $J = 3.9$ Hz), 122.70, 121.93 (d, $J = 5.5$ Hz), 116.96, 116.49, 116.27, 24.65, 14.32. ESI-HRMS m/z : 285.1155, $[M+1]^+$, calcd for C₁₅H₁₃FN₄O: 284.1073.

6d: Yellow powder, 72% yield. ¹H NMR (400 MHz, Chloroform-*d*, δ ppm) 8.53 (s, 1H), 8.47 (s, 1H), 8.18 (s, 1H), 7.79 (d, $J = 7.6$ Hz, 1H), 7.60 (d, $J = 7.4$ Hz, 1H), 7.56 (d, $J = 7.9$ Hz, 1H), 7.41 (d, $J = 7.4$ Hz, 1H), 2.62 (s, 3H), 2.29 (s, 3H).

¹³C NMR (101 MHz, Chloroform-*d*, δ ppm) 169.24, 162.94, 143.97, 137.57, 135.97, 132.46, 131.74, 128.60, 127.68 (q, $J = 265.7$ Hz), 126.49, 126.42, 125.38, 121.40, 117.50, 24.61, 14.32. ESI-HRMS m/z : 335.1121, $[M+1]^+$, calcd for C₁₆H₁₃F₃N₄O: 334.1041.

6e: White powder, 79% yield. ^1H NMR (400 MHz, Chloroform-*d*, δ ppm) 8.78 (d, $J = 1.4$ Hz, 1H), 8.39 (d, $J = 1.4$ Hz, 1H), 7.39 (t, $J = 7.9$ Hz, 1H), 7.32 (m, 1H), 7.18 (m, 1H), 7.12 (t, $J = 2.2$ Hz, 1H), 6.96 (m, 1H), 3.88 (s, 3H), 2.60 (s, 3H), 2.31 (s, 3H).

^{13}C NMR (101 MHz, Chloroform-*d*, δ ppm) 170.19, 162.43, 160.10, 143.68, 137.79, 130.18, 129.02, 126.00, 119.76, 119.59, 116.95, 113.79, 112.88, 55.32, 24.04, 14.06. ESI-HRMS m/z : 297.1353, $[\text{M}+1]^+$, calcd for $\text{C}_{16}\text{H}_{16}\text{N}_4\text{O}_2$: 296.1273.

6f: White powder, 82% yield. ^1H NMR (400 MHz, Chloroform-*d*, δ ppm) 8.75 (d, $J = 1.6$ Hz, 1H), 8.71 (s, 1H), 8.41 (d, $J = 1.6$ Hz, 1H), 7.72 (ddd, $J = 7.9, 1.8, 1.1$ Hz, 1H), 7.61 (t, $J = 7.8$ Hz, 1H), 7.52 (t, $J = 1.9$ Hz, 1H), 7.37 (ddd, $J = 8.0, 2.2, 1.1$ Hz, 1H), 3.76 (q, $J = 7.4$ Hz, 2H), 2.62 (s, 3H), 2.33 (s, 3H), 1.51 (t, $J = 7.4$ Hz, 3H).

^{13}C NMR (101 MHz, Chloroform-*d*, δ ppm) 171.21, 169.70, 163.11, 144.00, 138.84, 136.97, 130.74, 129.69, 128.82, 128.49, 127.07, 126.48, 120.02, 115.61, 49.43, 25.12, 24.62, 14.25, 8.21. ESI-HRMS m/z : 374.1302, $[\text{M}+1]^+$, calcd for $\text{C}_{17}\text{H}_{19}\text{N}_5\text{O}_3\text{S}$: 373.1209.

6g: Brown powder, 72% yield. ^1H NMR (400 MHz, Chloroform-*d*, δ ppm) 8.74 (d, $J = 1.6$ Hz, 1H), 8.56 (s, 1H), 8.39 (d, $J = 1.6$ Hz, 1H), 7.51 (m, 2H), 7.44 (m, 1H), 7.29 (m, 1H), 2.61 (s, 3H), 2.33 (s, 3H).

^{13}C NMR (101 MHz, DMSO-*d*₆, δ ppm) 170.68, 163.01, 149.45, 144.79, 139.16, 131.60, 127.03, 126.48, 125.58, 121.35, 120.83, 120.57 (q, $J = 257.4$ Hz), 119.94, 116.18, 24.37, 14.48.

ESI-HRMS m/z : 351.1067, $[\text{M}+1]^+$, calcd for $\text{C}_{16}\text{H}_{13}\text{F}_3\text{N}_4\text{O}_2$: 350.0991.

6h: White powder, 65% yield. ^1H NMR (400 MHz, Chloroform-*d*, δ ppm) 8.73 (d, $J = 1.6$ Hz, 1H), 8.42 (s, 1H), 8.38 (d, $J = 1.6$ Hz, 1H), 7.57 (m, 2H), 7.45 (d, $J = 8.1$ Hz, 2H), 3.74 (m, 4H), 3.57 (s, 2H), 2.61 (s, 3H), 2.49 (t, $J = 4.6$ Hz, 4H), 2.31 (s, 3H).

^{13}C NMR (101 MHz, DMSO-*d*₆, δ ppm) 170.62, 162.72, 144.54, 138.39, 135.44, 130.17, 127.17, 127.14, 126.92, 120.49, 116.44, 66.67, 62.44, 53.65, 24.41, 14.49. ESI-HRMS m/z : 366.1927, $[\text{M}+1]^+$, calcd for $\text{C}_{20}\text{H}_{23}\text{N}_5\text{O}_2$: 365.1852.

6i: White powder, 67% yield. ^1H NMR (400 MHz, Chloroform-*d*, δ ppm) 8.32 (s, 1H), 7.89 (d, $J = 0.84$ Hz, 1H), 7.47 (m, 4H), 7.25 (m, 1H), 7.22 (m, 2H), 7.18 (m, 2H), 2.54 (s, 3H), 2.29 (s, 3H).

^{13}C NMR (101 MHz, Chloroform-*d*, δ ppm) 168.90, 162.59, 149.83, 143.44, 141.15, 140.53, 135.50, 130.85, 130.72, 129.68, 125.26, 128.61, 128.53, 128.30, 127.79, 126.99, 125.30, 122.09, 118.42, 24.57, 14.29. ESI-HRMS m/z : 343.1563, $[\text{M}+1]^+$, calcd for $\text{C}_{21}\text{H}_{18}\text{N}_4\text{O}$: 342.4020.

6j: White powder, 87% yield. ^1H NMR (400 MHz, Chloroform-*d*, δ ppm) 8.66 (d, $J = 1.5$ Hz, 1H), 8.38 (d, $J = 1.5$ Hz, 1H), 8.34 (s, 1H), 7.36 (d, $J = 2.7$ Hz, 1H), 7.33 (m, 4H), 7.28 (m, 2H), 6.95 (d, $J = 8.8$ Hz, 1H), 5.11 (s, 2H), 2.60 (s, 3H), 2.30 (s, 3H).

¹³C NMR (101 MHz, Chloroform-*d*, δ ppm) 169.12, 162.76, 154.31, 144.73, 136.18, 130.54, 129.27, 128.60, 128.00, 127.84, 127.14, 126.35, 125.43, 124.25, 122.15, 117.86, 114.49, 100.00, 70.99, 24.61, 14.31. ESI-HRMS *m/z*: 407.1273, [M+1]⁺, calcd for C₂₂H₁₉ClN₄O₂: 406.1197.

6k: White powder, 85% yield. ¹H NMR (400 MHz, Chloroform-*d*, δ ppm) 8.69 (d, *J* = 1.6 Hz, 1H), 8.53 (s, 1H), 8.45 (d, *J* = 1.5 Hz, 1H), 7.20 (d, *J* = 2.3 Hz, 1H), 7.14 (dd, *J* = 8.5, 2.2 Hz, 1H), 6.89 (d, *J* = 8.3 Hz, 1H), 4.07 (q, *J* = 6.9 Hz, 2H), 2.60 (s, 3H), 2.34 (s, 3H), 2.30 (s, 3H), 1.37 (t, *J* = 7.0 Hz, 3H).

¹³C NMR (101 MHz, Chloroform-*d*, δ ppm) 169.20, 162.45, 153.80, 131.31, 130.28, 129.97, 125.61, 125.38, 125.15, 122.20, 118.71, 112.54, 64.25, 24.61, 20.48, 14.77, 14.27. ESI-HRMS *m/z*: 325.1658, [M+1]⁺, calcd for C₁₇H₁₈ClN₄O₂: 324.1586.

6l: White powder, 88% yield. ¹H NMR (400 MHz, Chloroform-*d*, δ ppm) 8.69 (d, *J* = 1.5 Hz, 1H), 8.53 (s, 1H), 8.45 (d, *J* = 1.5 Hz, 1H), 7.19 (d, *J* = 2.2 Hz, 1H), 7.14 (dd, *J* = 7.9, 2.1 Hz, 1H), 6.89 (d, *J* = 8.3 Hz, 1H), 4.06 (q, *J* = 7.0 Hz, 2H), 2.60 (s, 3H), 2.34 (s, 3H), 2.30 (s, 3H), 1.37 (t, *J* = 7.0 Hz, 3H).

¹³C NMR (101 MHz, Chloroform-*d*, δ ppm) 169.22, 162.44, 153.79, 143.65, 131.31, 130.28, 129.97, 125.61, 125.37, 125.15, 122.20, 118.76, 112.53, 64.25, 24.60, 20.48, 14.77, 14.26. ESI-HRMS *m/z*: 325.1658, [M+1]⁺, calcd for C₁₈H₂₀N₄O₂: 324.1586.

6m: White powder, 82% yield. ¹H NMR (400 MHz, Chloroform-*d*, δ ppm) 8.69 (d, *J* = 1.6 Hz, 1H), 8.53 (s, 1H), 8.45 (d, *J* = 1.5 Hz, 1H), 7.20 (d, *J* = 2.3 Hz, 1H), 7.14 (dd, *J* = 8.5, 2.2 Hz, 1H), 6.89 (d, *J* = 8.3 Hz, 1H), 4.07 (q, *J* = 6.9 Hz, 2H), 2.60 (s, 3H), 2.34 (s, 3H), 2.30 (s, 3H), 1.37 (t, *J* = 7.0 Hz, 3H).

¹³C NMR (101 MHz, Chloroform-*d*, δ ppm) 169.01, 162.82, 154.74, 141.03, 130.35, 129.20, 127.27, 125.76, 125.31, 124.25, 122.20, 117.82, 113.55, 70.50, 24.66, 22.39, 14.35, 10.58. ESI-HRMS *m/z*: 359.1278, [M+1]⁺, calcd for C₁₈H₁₉ClN₄O₂: 358.1197.

6n: White powder, 77% yield. ¹H NMR (400 MHz, Chloroform-*d*, δ ppm) 8.64 (d, *J* = 1.5 Hz, 1H), 8.38 (d, *J* = 1.5 Hz, 1H), 8.35 (s, 1H), 7.33 (dd, *J* = 8.4, 6.6 Hz, 1H), 6.74 (m, 2H), 4.08 (q, *J* = 7.0 Hz, 2H), 2.61 (s, 3H), 2.30 (s, 3H), 1.41 (t, *J* = 7.0 Hz, 3H).

¹³C NMR (101 MHz, Chloroform-*d*, δ ppm) 169.09, 162.63(d, *J* = 254.5 Hz), 157.16, 157.06, 143.72, 131.56, 131.46, 125.21, 124.79, 121.95, 118.32, 107.43 (d, *J* = 21.5 Hz), 100.44, 64.48, 24.66, 14.50, 14.32. ESI-HRMS *m/z*: 329.1411, [M+1]⁺, calcd for C₁₇H₁₇FN₄O₂: 328.1336.

6o: Off-white powder, 77% yield. ¹H NMR (400 MHz, Chloroform-*d*, δ ppm) 8.75 (s, 1H), 8.69 (d, *J* = 1.5 Hz, 1H), 8.56 (d, *J* = 1.5 Hz, 1H), 8.21 (dd, *J* = 4.9, 1.8 Hz, 1H), 7.73 (dd, *J* = 7.4, 1.8 Hz, 1H), 7.02 (dd, *J* = 7.4, 4.9 Hz, 1H), 4.01 (s, 3H), 2.61 (s, 3H), 2.3 (s, 3H).

^{13}C NMR (101 MHz, Chloroform-*d*, δ ppm) 169.55, 162.76, 160.72, 146.75, 143.77, 138.66, 125.72, 123.54, 122.39, 119.75, 117.66, 117.29, 53.74, 29.69, 14.19. ESI-HRMS m/z : 298.1301, $[\text{M}+1]^+$, calcd for $\text{C}_{15}\text{H}_{15}\text{N}_5\text{O}_2$: 297.1226.

6p: White powder, 65% yield. ^1H NMR (400 MHz, Chloroform-*d*, δ ppm) 8.67 (d, $J = 1.4$ Hz, 1H), 8.39 (d, $J = 1.4$ Hz, 1H), 8.26 (s, 1H), 7.35 (dd, $J = 8.3, 6.7$ Hz, 1H), 6.72 (ddd, $J = 10.2, 7.6, 4.0$ Hz, 2H), 4.07 (q, $J = 7.0$ Hz, 2H), 2.61 (s, 3H), 2.40 (tt, $J = 11.7, 4.1$ Hz, 1H), 2.01 (d, $J = 12.9$ Hz, 2H), 1.86 (d, $J = 11.8$ Hz, 2H), 1.73 (d, $J = 10.0$ Hz, 2H), 1.56 (d, $J = 11.7$ Hz, 2H), 1.40 (t, $J = 7.0$ Hz, 3H), 1.29 (m, 2H).

^{13}C NMR (101 MHz, Chloroform-*d*, δ ppm) 175.93, 162.67, 159.94 (d, $J = 247.4$ Hz), 157.01, 143.96, 131.91, 124.60, 121.75, 118.02, 117.82, 100.57, 100.29, 99.98, 64.49, 46.44, 29.58 (2C), 25.62, 25.58 (2C), 14.52, 14.36. ESI-HRMS m/z : 397.2042, $[\text{M}+1]^+$, calcd for $\text{C}_{22}\text{H}_{25}\text{F}_3\text{N}_4\text{O}_2$: 396.1962.

6q: White powder, 69% yield. ^1H NMR (400 MHz, Chloroform-*d*, δ ppm) 8.72 (d, $J = 1.6$ Hz, 1H), 8.58 (d, $J = 1.6$ Hz, 1H), 8.49 (s, 1H), 8.20 (dd, $J = 4.9, 1.9$ Hz, 1H), 7.75 (dd, $J = 7.4, 1.9$ Hz, 1H), 7.00 (dd, $J = 7.3, 5.0$ Hz, 1H), 4.01 (s, 3H), 2.61 (s, 3H), 2.44 (m, 1H), 2.01 (m, 3H), 1.86 (m, 2H), 1.72 (m, 1H), 1.60 (m, 2H), 1.37 (m, 2H).

^{13}C NMR (101 MHz, Chloroform-*d*, δ ppm) 175.67, 162.84, 160.68, 146.66, 143.95, 138.68, 125.88, 123.36, 122.27, 119.79, 117.25, 53.75, 46.32, 29.56 (2C), 25.58 (2C), 14.28. ESI-HRMS m/z : 366.1926, $[\text{M}+1]^+$, calcd for $\text{C}_{22}\text{H}_{25}\text{F}_3\text{N}_4\text{O}_2$: 365.1852.

4.1.5. General Procedure for the Preparation of 7a–k

A mixture of compound **4** (2 mmol), boric acids or borates (2.4 mmol), [1,1'-bis(diphenylphosphino)ferrocene]dichloropalladium(II) (**5 mol %**), and sodium carbonate (6 mmol) in 1,4-dioxane (8 mL) and water (4 mL) was heated under nitrogen conditions (90 °C, 6 h). After cooling to ambient temperature, the reaction mixture was filtered and concentrated. The residue was partitioned between the water and dichloromethane. The aqueous layer was extracted with dichloromethane three additional times. The combined organic layers were washed with saturated aqueous sodium chloride, dried over anhydrous sodium sulfate, filtered, and concentrated. The residue was purified by flash chromatography to provide compounds **5a–k**.

To a cold (0 °C) stirred solution of each individual compound **5a–k** (1 mmol) in dry dichloromethane (5 mL) was added pyridine (1.5 mmol) followed by ethanesulfonyl chloride (1.5 mmol). The reaction mixture was stirred at room temperature. Upon completion (TLC), the reaction mixture was evaporated to dryness under vacuum. The residue was diluted with H_2O (20 mL) and dichloromethane (20 mL). The organic layer was washed with H_2O and brine, and the

combined extracts were dried over Na_2SO_4 , filtered and concentrated under reduced pressure, then purified by flash chromatography on silica gel to give the desired compounds⁴¹.

7a: Light yellow powder, 68% yield. ^1H NMR (400 MHz, Chloroform-*d*, δ ppm) 8.44 (d, $J = 1.5$ Hz, 1H), 7.87 (d, $J = 1.5$ Hz, 1H), 7.57 (m, 2H), 7.50 (m, 2H), 7.44 (m, 1H), 3.24 (q, $J = 7.4$ Hz, 2H), 2.61 (s, 3H), 1.43 (t, $J = 7.4$ Hz, 3H).

^{13}C NMR (101 MHz, DMSO-*d*₆, δ ppm) 163.24, 146.23, 136.21, 129.66 (2C), 128.70, 127.41 (2C), 127.10, 126.20, 122.32, 119.80, 47.62, 14.63, 8.61. ESI-HRMS m/z : 317.1073, $[\text{M}+1]^+$, calcd for $\text{C}_{15}\text{H}_{16}\text{F}_3\text{N}_4\text{O}_2\text{S}$: 316.0994.

7b: White powder, 54% yield. ^1H NMR (400 MHz, Chloroform-*d*, δ ppm) 8.39 (d, $J = 1.5$ Hz, 1H), 7.79 (d, $J = 1.5$ Hz, 1H), 7.44 (d, $J = 6.6$ Hz, 2H), 7.32 (s, 1H), 7.21 (m, 1H), 3.18 (q, $J = 7.4$ Hz, 2H), 2.52 (s, 3H), 1.35 (t, $J = 7.4$ Hz, 3H).

^{13}C NMR (101 MHz, DMSO-*d*₆, δ ppm) 163.50, 149.46, 146.46, 138.65, 131.61, 126.62, 126.27, 125.44, 123.08, 120.96, 120.58 (q, $J = 257.3$ Hz), 120.16, 119.67, 47.67, 14.63, 8.59. ESI-HRMS m/z : 385.0944, $[\text{M}+1]^+$, calcd for $\text{C}_{16}\text{H}_{15}\text{F}_3\text{N}_4\text{O}_2\text{S}$: 384.0868.

7c: White powder, 59% yield. ^1H NMR (400 MHz, Chloroform-*d*, δ ppm) 8.46 (d, $J = 1.5$ Hz, 1H), 7.84 (d, $J = 1.5$ Hz, 1H), 7.45 (m, 2H), 7.34 (d, $J = 8.0$ Hz, 2H), 7.31 (s, 1H), 3.24 (m, 4H), 2.60 (s, 3H), 1.43 (q, $J = 7.5$ Hz, 6H).

^{13}C NMR (101 MHz, Chloroform-*d*, δ ppm) 163.67, 144.52, 138.10, 137.78, 130.64, 127.61, 125.65, 123.55, 120.87, 119.87, 118.69, 115.53, 47.14, 46.43, 29.70, 14.31, 8.27. ESI-HRMS m/z : 424.1116, $[\text{M}+1]^+$, calcd for $\text{C}_{15}\text{H}_{17}\text{N}_5\text{O}_3\text{S}$: 423.1035.

7d: Yellow powder, 61% yield. ^1H NMR (400 MHz, Chloroform-*d*, δ ppm) 8.22 (s, 1H), 7.81 (d, $J = 7.8$ Hz, 1H), 7.60 (td, $J = 15.1, 13.5, 7.4$ Hz, 3H), 7.41 (d, $J = 7.5$ Hz, 1H), 3.23 (q, $J = 7.4$ Hz, 2H), 2.62 (s, 3H), 1.41 (t, $J = 7.3$ Hz, 3H).

^{13}C NMR (101 MHz, DMSO-*d*₆, δ ppm) δ 163.38, 145.96, 135.83, 133.27, 133.09, 129.61, 126.79, 126.74, 125.84, 125.59, 125.43, 124.38 (q, $J = 258.9$ Hz), 123.69, 123.67, 123.01, 120.61, 120.47, 120.46, 47.40, 14.56, 8.53. ESI-HRMS m/z : 385.0944, $[\text{M}+1]^+$, calcd for $\text{C}_{16}\text{H}_{15}\text{F}_3\text{N}_4\text{O}_2\text{S}$: 384.0868.

7e: White powder, 74% yield. ^1H NMR (400 MHz, Chloroform-*d*, δ ppm) 8.25 (d, $J = 1.5$ Hz, 1H), 7.64 (d, $J = 1.4$ Hz, 1H), 7.45 (ddt, $J = 7.1, 5.0, 3.5$ Hz, 1H), 7.31 (m, 3H), 3.19 (q, $J = 7.4$ Hz, 2H), 2.54 (s, 3H), 1.36 (t, $J = 7.4$ Hz, 3H).

^{13}C NMR (101 MHz, Chloroform-*d*, δ ppm) 162.50, 143.21, 134.12, 131.98, 130.34, 129.35, 129.00, 126.36, 125.17, 123.97, 121.64, 116.19, 45.87, 28.68, 13.24. ESI-HRMS m/z : 351.0712, $[\text{M}+1]^+$, calcd for $\text{C}_{15}\text{H}_{15}\text{ClN}_4\text{O}_2\text{S}$: 350.0621.

7f: Light yellow powder, 52% yield. ^1H NMR (400 MHz, Chloroform-*d*, δ ppm) 8.24 (s, 1H), 7.54 (m, 5H), 7.25 (m, 6H), 3.40 (m, 2H), 2.58 (s, 3H), 1.19 (t, $J = 7.3$ Hz, 3H).

^{13}C NMR (101 MHz, DMSO-*d*₆, δ ppm) 162.98, 144.99, 140.81, 140.72, 135.49, 131.33, 131.17, 129.95 (2C), 129.23, 128.85 (2C), 128.42, 127.77, 127.47, 125.33, 123.39, 120.02, 46.36, 14.50, 8.40. ESI-HRMS m/z : 393.1383, $[\text{M}+1]^+$, calcd for $\text{C}_{21}\text{H}_{20}\text{N}_4\text{O}_2\text{S}$: 392.1307.

7g: White powder, 46% yield. ^1H NMR (400 MHz, Chloroform-*d*, δ ppm) 8.40 (d, $J = 1.4$ Hz, 1H), 7.85 (d, $J = 1.4$ Hz, 1H), 7.34 (m, 7H), 7.09 (m, 2H), 5.11 (s, 2H), 2.98 (q, $J = 7.4$ Hz, 2H), 2.59 (s, 3H), 1.26 (t, $J = 7.4$ Hz, 4H).

^{13}C NMR (101 MHz, Chloroform-*d*, δ ppm) 163.21, 155.83, 144.15, 136.44, 130.78, 130.08, 128.65 (2C), 128.08, 127.55 (2C), 125.63, 122.44, 121.53, 117.78, 112.92, 70.66, 46.13, 14.30, 8.36. ESI-HRMS m/z : 423.1492, $[\text{M}+1]^+$, calcd for $\text{C}_{22}\text{H}_{22}\text{N}_4\text{O}_3\text{S}$: 422.1413.

7h: White powder, 56% yield. ^1H NMR (400 MHz, Chloroform-*d*, δ ppm) 8.45 (d, $J = 1.5$ Hz, 1H), 7.83 (d, $J = 1.4$ Hz, 1H), 7.18 (m, 2H), 6.91 (d, $J = 8.3$ Hz, 1H), 3.82 (s, 3H), 3.23 (q, $J = 7.4$ Hz, 2H), 2.60 (s, 3H), 2.35 (s, 3H), 1.42 (t, $J = 7.4$ Hz, 3H).

^{13}C NMR (101 MHz, Chloroform-*d*, δ ppm) 163.23, 154.40, 144.22, 131.10, 130.55, 130.32, 125.16, 124.69, 124.43, 123.01, 118.28, 111.42, 55.70, 46.60, 20.47, 14.31, 8.35. ESI-HRMS m/z : 361.1331, $[\text{M}+1]^+$, calcd for $\text{C}_{17}\text{H}_{20}\text{N}_4\text{O}_3\text{S}$: 360.1256.

7i: White powder, 62% yield. ^1H NMR (400 MHz, Chloroform-*d*, δ ppm) 8.31 (d, $J = 1.5$ Hz, 1H), 7.76 (d, $J = 1.5$ Hz, 1H), 7.23 (dd, $J = 8.4, 6.6$ Hz, 1H), 6.73 – 6.63 (m, 2H), 4.00 (q, $J = 7.0$ Hz, 2H), 3.16 (q, $J = 7.4$ Hz, 2H), 2.53 (s, 3H), 1.35 (td, $J = 7.2, 3.2$ Hz, 6H).

^{13}C NMR (101 MHz, Chloroform-*d*, δ ppm) 163.79 (d, $J = 249.1$ Hz), 163.32, 157.14 (d, $J = 10.0$ Hz), 144.28, 131.35 (d, $J = 10.1$ Hz), 124.74, 124.41, 122.67, 121.04 (d, $J = 3.4$ Hz), 118.22, 107.54 (d, $J = 21.6$ Hz), 100.45 (d, $J = 25.8$ Hz), 64.44, 46.64, 14.50, 14.30, 8.33. ESI-HRMS m/z : 379.1241, $[\text{M}+1]^+$, calcd for $\text{C}_{17}\text{H}_{19}\text{FN}_4\text{O}_3\text{S}$: 378.1162.

7j: White powder, 55% yield. ^1H NMR (400 MHz, Chloroform-*d*, δ ppm) 8.36 (d, $J = 1.4$ Hz, 1H), 7.77 (d, $J = 1.4$ Hz, 1H), 7.33 (m, 7H), 7.00 (d, $J = 9.5$ Hz, 1H), 5.08 (s, 2H), 2.97 (q, $J = 7.4$ Hz, 2H), 2.60 (s, 3H), 1.27 (t, $J = 7.2$ Hz, 3H).

^{13}C NMR (101 MHz, Chloroform-*d*, δ ppm) 163.41, 154.43, 135.95, 130.40, 129.63, 128.72, 128.26, 127.55, 127.20, 126.41, 124.62, 124.32, 122.45, 116.96, 114.25, 71.07, 46.23, 14.33, 8.35. ESI-HRMS m/z : 457.1099, $[\text{M}+1]^+$, calcd for $\text{C}_{22}\text{H}_{21}\text{ClN}_4\text{O}_3\text{S}$: 456.1023.

7k: White powder, 59% yield. ^1H NMR (400 MHz, Chloroform-*d*, δ ppm) 8.58 (d, $J = 1.5$ Hz, 1H), 8.23 (dd, $J = 5.0, 1.9$ Hz, 1H), 7.88 (d, $J = 1.5$ Hz, 1H), 7.70 (dd, $J = 7.4, 1.9$ Hz, 1H), 7.03 (dd, $J = 7.4, 5.0$ Hz, 1H), 4.01 (s, 3H), 3.24 (q, $J = 7.4$ Hz, 2H), 2.61 (s, 3H), 1.42 (t, $J = 7.4$ Hz, 3H).

^{13}C NMR (101 MHz, Chloroform-*d*, δ ppm) 163.30, 160.65, 147.11, 144.20, 138.49, 125.12, 123.53, 123.11, 119.20, 117.75, 117.41, 53.80, 46.97, 14.10, 8.32. ESI-HRMS m/z : 348.1146, $[\text{M}+1]^+$, calcd for $\text{C}_{15}\text{H}_{17}\text{N}_5\text{O}_3\text{S}$: 347.1052.

4.1.6. General Procedure for the Preparation of **8a–f**

A mixture of compound **4** (2 mmol), boric acids or borates (2.4 mmol), [1,1'-bis(diphenylphosphino)ferrocene]dichloropalladium(II) (**5 mol %**), and sodium carbonate (6 mmol) in 1,4-dioxane (8 mL) and water (4 mL) was heated under nitrogen conditions (90 °C, 6 h). After cooling to ambient temperature, the reaction mixture was filtered and concentrated. The residue was partitioned between water and dichloromethane. The aqueous layer was extracted with dichloromethane three additional times. The combined organic layers were washed with saturated aqueous sodium chloride, dried over anhydrous sodium sulfate, filtered, and concentrated. The residue was purified by flash chromatography to provide compounds **5a–f**.

We added aromatic acid chloride (1.5 mmol) dropwise to a solution of each individual compound **5a–f** (1 mmol), anhydrous dichloromethane (5 mL) and potassium carbonate (1.5 mmol) at 0 °C under stirring. We stirred the mixture at room temperature for 1 h until TLC showed the reaction was complete. The reaction mixture was diluted with dichloromethane and washed with water. The organic extract was dried, concentrated and purified by column chromatography using silica gel to give the compounds **8a–f** as off-white solids⁴⁰.

8a: White powder, 82% yield. ^1H NMR (400 MHz, Chloroform-*d*, δ ppm) 9.00 (s, 1H), 8.86 (d, $J = 1.7$ Hz, 1H), 8.41 (d, $J = 1.6$ Hz, 1H), 8.05 (m, 2H), 7.58 (m, 2H), 7.48 (m, 2H), 7.23 (t, $J = 8.6$ Hz, 2H), 2.63 (s, 3H).

^{13}C NMR (101 MHz, Chloroform-*d*, δ ppm) 129.91, 129.82, 129.42, 128.48, 119.80, 116.24, 116.02, 115.60, 14.39. ESI-HRMS m/z : 381.0927, $[\text{M}+1]^+$, calcd for $\text{C}_{20}\text{H}_{14}\text{ClFN}_4\text{O}$: 380.0840.

8b: White powder, 84% yield. ^1H NMR (400 MHz, Chloroform-*d*, δ ppm) 9.15 (s, 1H), 8.87 (d, $J = 1.7$ Hz, 1H), 8.43 (d, $J = 1.6$ Hz, 1H), 8.31 (s, 1H), 8.20 (d, $J = 7.8$ Hz, 1H), 7.87 (d, $J = 7.8$ Hz, 1H), 7.69 (t, $J = 7.9$ Hz, 1H), 7.60 – 7.54 (m, 2H), 7.47 (d, $J = 8.5$ Hz, 2H), 2.63 (s, 3H).

^{13}C NMR (101 MHz, Chloroform-*d*, δ ppm) 164.84, 163.27, 144.26, 135.00, 134.69, 134.54, 131.82, 131.49, 130.39, 129.57, 129.45, 129.09 (d, $J = 3.6$ Hz), 128.45, 126.83, 126.01, 125.98 (q, $J = 253.1$ Hz), 124.70, 124.66, 120.12, 116.14, 14.35. ESI-HRMS m/z : 431.0883, $[\text{M}+1]^+$, calcd for $\text{C}_{21}\text{H}_{14}\text{ClF}_3\text{N}_4\text{O}$: 430.0808.

8c: White powder, 76% yield. ^1H NMR (400 MHz, Chloroform-*d*, δ ppm) 9.55 (d, $J = 14.6$ Hz, 1H), 8.80 (d, $J = 1.5$ Hz, 1H), 8.47 (d, $J = 1.5$ Hz, 1H), 8.16 (td, $J = 7.9, 1.9$ Hz, 1H), 7.58 (q, $J =$

6.9, 6.2 Hz, 1H), 7.41 (d, $J = 2.6$ Hz, 1H), 7.34 (m, 2H), 6.93 (d, $J = 8.8$ Hz, 1H), 3.97 (t, $J = 6.5$ Hz, 2H), 2.64 (s, 3H), 1.79 (q, $J = 7.0$ Hz, 2H), 0.96 (t, $J = 7.4$ Hz, 3H).

^{13}C NMR (101 MHz, Chloroform-*d*, δ ppm) 172.39, 169.24, 156.72 (d, $J = 260.1$ Hz), 149.30, 137.40, 135.57, 130.23, 129.14, 128.25, 125.64, 123.91, 122.59, 121.73, 118.23, 114.62, 108.92, 99.98, 50.22, 24.26, 22.34, 10.53. ESI-HRMS m/z : 439.1342, $[\text{M}+1]^+$, calcd for $\text{C}_{23}\text{H}_{20}\text{ClFN}_4\text{O}_2$: 438.1259.

8d: White powder, 74% yield. ^1H NMR (400 MHz, Chloroform-*d*, δ ppm) 8.88 (s, 1H), 8.77 (d, $J = 1.5$ Hz, 1H), 8.47 (d, $J = 1.5$ Hz, 1H), 7.97 (m, 2H), 7.18 (dd, $J = 8.9, 3.1$ Hz, 1H), 7.07 (m, 1H), 7.01 (t, $J = 3.0, 2.0$ Hz, 1H), 6.99 (t, $J = 2.0, 3.0$ Hz, 1H), 6.95 (dd, $J = 9.1, 4.5$ Hz, 1H), 4.13 (q, $J = 7.0$ Hz, 2H), 3.84 (s, 3H), 2.63 (s, 3H), 1.47 (t, $J = 7.0$ Hz, 3H).

^{13}C NMR (101 MHz, Chloroform-*d*, δ ppm) 165.58, 163.00, 163.33 (d, $J = 253.9$ Hz), 158.29, 152.81 (d, $J = 2.1$ Hz), 144.30, 129.31, 125.86, 125.80, 124.15, 122.27, 117.58, 117.48, 117.34, 115.60, 115.38, 114.57, 112.48, 112.40, 63.82, 56.26, 14.69, 14.40. ESI-HRMS m/z : 421.1675, $[\text{M}+1]^+$, calcd for $\text{C}_{23}\text{H}_{21}\text{FN}_4\text{O}_3$: 420.1598.

8e: White powder, 57% yield. ^1H NMR (400 MHz, Chloroform-*d*, δ ppm) 8.87 (s, 1H), 8.80 (s, 1H), 8.52 (s, 1H), 7.47 (m, 1H), 7.19 (dd, $J = 8.8, 3.1$ Hz, 1H), 7.06 (m, 3H), 6.96 (dd, $J = 9.0, 4.5$ Hz, 1H), 3.85 (s, 3H), 2.61 (s, 3H).

^{13}C NMR (101 MHz, Chloroform-*d*, δ ppm) 165.46, 161.86 (d, $J = 243.2$ Hz), 161.36, 159.06, 152.80, 137.54, 137.12, 132.82, 132.72, 132.62, 131.53 (d, $J = 5.1$ Hz), 131.31, 125.05, 124.13, 123.10, 118.45, 117.56, 117.32, 115.78, 115.55, 112.48 (d, $J = 7.8$ Hz), 112.19, 99.99, 56.25, 14.34. ESI-HRMS m/z : 413.1222, $[\text{M}+1]^+$, calcd for $\text{C}_{21}\text{H}_{15}\text{F}_3\text{N}_4\text{O}_2$: 412.1147.

8f: White powder, 71% yield. ^1H NMR (400 MHz, Chloroform-*d*, δ ppm) 8.99 (s, 1H), 8.77 (d, $J = 1.5$ Hz, 1H), 8.48 (d, $J = 1.5$ Hz, 1H), 8.09 (d, $J = 8.0$ Hz, 2H), 8.04 (d, $J = 8.0$ Hz, 1H), 7.98 (d, $J = 8.0$ Hz, 2H), 7.36 (d, $J = 8.0$ Hz, 2H), 7.18 (dd, $J = 8.8, 3.1$ Hz, 1H), 7.03 (d, $J = 4.0$ Hz, 2H), 6.95 (dd, $J = 9.1, 4.5$ Hz, 1H), 5.16 (s, 2H), 3.84 (s, 3H), 2.63 (s, 3H).

^{13}C NMR (101 MHz, Chloroform-*d*, δ ppm) 165.65, 163.71, 161.78 (d, $J = 244.9$ Hz), 162.94, 162.16 (d, $J = 10.2$ Hz), 136.18, 135.92, 132.85, 132.27, 129.40, 128.75 (2C), 128.72, 128.70, 128.35, 128.26, 128.24, 127.50 (2C), 125.82, 122.37, 121.50, 117.93, 114.98, 114.56, 70.30, 56.25, 14.33. ESI-HRMS m/z : 517.1445, $[\text{M}+1]^+$, calcd for $\text{C}_{28}\text{H}_{22}\text{ClFN}_4\text{O}_3$: 516.1364.

4.2 Biology experiments

4.2.1. Reagents

Compound **8d** was dissolved in dimethyl sulfoxide (DMSO) and stored at -20 °C. 3-(4,5-dimethyl-2-thiazolyl)-2,5-diphenyl-2H-tetrazolium bromide (MTT), PEG400, Con A and

LPS were purchased from Sigma-Aldrich (St. Louis, MO, USA). 4',6-diamidino-2-phenylindole (DAPI) was purchased from Beyotime (Shanghai, China). The primary antibody P65 was purchased from Proteintech (Wuhan, China). PE-CD11b and FITC-Gr-1 conjugated antibodies were obtained from BD Biosciences (San Diego, CA, USA). Rabbit polyclonal anti-CD4, rabbit polyclonal anti-CD11b and rabbit polyclonal anti-F4/80 were purchased from Merck Millipore. For the *in vivo* experiments, compound **8d** was prepared in 40% (v/v) PEG 400 and 60% (v/v) saline.

4.2.2. Cell lines and cell cultivation

RAW264.7 cells and human liver cells LO₂ were purchased from the American Type Culture Collection (ATCC, Rockville, MD, USA). Both of them were cultured in DMEM media supplemented with 10% fetal bovine serum and 1% antibiotics (penicillin and streptomycin). Cells were cultivated in a humidified environment with 5% CO₂ at 37 °C.

4.2.3. Cell viability assay

The effect of all synthesized compounds on cell viability was estimated by an MTT assay. In brief, LO₂ cells ($1.5-5 \times 10^3$) were seeded in 96-well plates and incubated overnight. After that, compounds were used to treat the cells for 24 h. Then, 20 μ L MTT (5 mg/mL) solution was added to each well and incubated with the cells for 2-4 h at 37 °C. All of the medium was removed and 150 μ L of DMSO was added for 10 min. The absorbance was measured at 570 nm using a Spectra MAX M5 microplate spectrophotometer (Molecular Devices, CA, USA). Each experiment was replicated three times.

4.2.4. Measurement of NO release

RAW264.7 cells (1×10^5 /mL) were seeded in 96-well plates and incubated overnight. Then, the cells were treated with the tested compounds for 1 h. Next, 1 μ g/mL LPS was added for another 23 h. Briefly, the culture supernatants were harvested for measurement of NO production using the Griess reagent (Beyotime, Shanghai, China) at an optical density of 540 nm.

4.2.5. Chemotaxis assay

RAW264.7 cells were starved for 3 h in serum-free medium. Transwell cell chambers containing a polycarbonate filter were used in this assay. In the upper chamber, 200 μ L of medium that included RAW264.7 cells with 0.5% BSA and 20 μ M compounds or DMSO were added. Then, 600 μ L DMEM medium with 200 ng/mL MCP-1 (R&D, USA) was added to the lower chamber. After incubation at 37 °C for 3 h, nonmigratory cells were discarded from the upper surface of the filter using a cotton swab. Then, the filters were washed in PBS three times. The migrated cells were fixed with 4% paraformaldehyde for 1 h and stained with a 0.5% crystal violet solution (Beyotime, Shanghai, China) for 15 min. We randomly selected visual fields and counted

and photographed the migrating cells under a light microscope. The standard deviation of the average was calculated by three replicated chambers.

$$\text{Inhibitory rates} = 1 - N_1 / (N_1 + N_2)$$

N_1 = the number of migratory cells; N_2 = the number of nonmigratory cells; Eight different areas of migrated cells were counted for each well ($n = 3$) and the inhibitory rates were expressed as the mean \pm SD ($p < 0.05$).

4.2.6. Immunofluorescence assay

The concentration of Con A used in this study was in accordance with that previously described⁴². RAW264.7 macrophages (2×10^4 /well) were seeded in 24-well plates and incubated overnight. Cells were pretreated with Con A or LPS for 2 h. Then, the cells were treated with different concentration of compound **8d** for another 22 h. Subsequently, the cells were washed three times in PBS and fixed in 4% paraformaldehyde for 10 min and washed three times in PBS. Then, the cells were penetrated with PBS solution containing 0.5% Triton X-100 for 10 min and washed three times. After incubation with PBST containing 5% BSA and 0.05% Triton X-100 (blocking solution) for 30 min, the cells were incubated with primary antibody overnight at 4 °C. Goat anti-rabbit secondary antibodies conjugated to FITC were used. Cell nuclei were stained with DAPI. Photographs were taken using a laser-scanning confocal microscopy (Nikon).

4.2.7. Preparation of RNA and real-time PCR

The total RNA from liver tissues and RAW264.7 cells were isolated using Trizol reagent (Thermo Fisher Scientific, Inc.). Total RNA (3 μ g) was reverse transcribed to cDNA by using an M5 First Strand cDNA Synthesis Kit (Mei5 Biotechnology, Beijing, China) according to the manufacturer's protocol. Real-time PCRs were performed using SYBR Premix Ex Taq II (Takara, Kusatsu, Japan), and the conditions of this assay were performed as follows: 95 °C for 30 s, the following 40 cycles including 95 °C for 5 s and 60 °C for 20 s. All PCR assays were performed in triplicate. Expression of mRNA was normalized to GAPDH expression. The following primers were used:

GAPDH: MF TTGCGACTTCAACAGCAACTC; MR GGTCTGGGATGGAAATTGTG,
 TNF- α : MF GGCAGGTCTACTTTGGAGTCAT; MR CAGAGTAAAGGGGTCAGAGTGG,
 IFN- γ : MF CAGCAACAGCAAGGCGAAA; MR CTGGACCTGTGGGTTGTTGAC,
 IL-6: MF AACCACGGCCTTCCCTACTT; MR TTGGGAGTGGTATCCTCTGTGA,
 IL-10: MF GATGCCCCAGGCAGAGAA; MR CACCCAGGGAATTCAAATGC

4.2.8. Flow cytometry

Single-cell suspensions of livers were made by mechanical and enzymatic dispersion as described previously⁴³. Briefly, red blood cells were lysed and washed twice using PBS. The

single-cell suspensions of the liver were acquired by mechanical disruption and 1 mg/mL collagenase I digestion. Then, 1×10^6 freshly prepared cells were suspended in 100 μ L of PBS and stained with different combinations of fluorochrome-coupled antibodies for CD11b and Gr-1. The cells were collected by FCM, and the data were analyzed by FlowJo software.

4.2.9. Animals

All animal experiments complied with the National Institutes of Health guide for the care and use of laboratory animals (NIH Publications No. 8023, revised 1978). Six to eight weeks old female BALB/c mice (HFK bioscience CO., LTD, Beijing, China) were used in this study. The mice were housed in an SPF environment. The experiments were approved and conducted in accordance with the Animal Care and Use Committee of Sichuan University. This model was established as previously described⁹. The mice were randomly divided into three groups: control (pathogen-free saline), Con A (20 mg/kg) and compound **8d** (100 mg/kg). The control group mice were administered pathogen-free saline by intravenous injection and the Con A group were given Con A 20 mg/kg followed by the administered solvent (40% (v/v) PEG 400 and 60% (v/v) saline) by intraperitoneal injection. The compound **8d** group mice were given Con A 20 mg/kg followed by the administered **8d** (100 mg/kg). After 12 h, the mice were sacrificed and serum and liver tissue were collected for subsequent experiments.

4.2.10. Liver function assessment

Blood samples were centrifuged at 3000 rpm for 10 min to collect the plasma. Levels of ALT and AST were measured on an automatic analyzer (Hitachi Auto Analyzer 7170, Japan).

4.2.11. Histopathology and immunohistochemistry

Liver sections were fixed in 4% formalin, embedded in paraffin, dehydrated with 70% ethanol, and cut into 4–5 μ m slices. The slices were stained with hematoxylin and eosin (H&E) and examined under a light microscope to analyze hepatic changes. In addition the liver tissue sections were stained with primary antibodies (CD4, CD11b and F4/80). Images were taken using a fluorescence microscope (Olympus, Tokyo, Japan).

4.2.12. Statistical analysis

Results are expressed as the mean values and standard deviation (SD) and were analyzed statistically with analysis of variance (ANOVA), and differences between groups were assessed with Tukey's method. A value of $p < 0.05$ was considered statistically significant.

Notes

The authors declare no competing financial interest.

Declarations of interest: none.

Acknowledgments

The authors acknowledge the National Natural Science Foundation of China (No.81873580), the Key Project of the Science & Technology Department of Sichuan Province (Grant No. 2017JY0071), the National S&T Major Special Project on Major New Drug Innovations (2018ZX09201018), and 1.3.5 project for disciplines of excellence, West China Hospital, Sichuan University (ZYJC18008).

Supplementary data

Supplementary data include ¹HNMR and ¹³CNMR of the compounds described in this article.

References

1. Coussens, L. M.; Werb, Z., Inflammation and cancer. *Nature* **2002**, *420* (6917), 860-7.
2. Baumgart, D. C.; Carding, S. R., Inflammatory bowel disease: cause and immunobiology. *Lancet* **2007**, *369* (9573), 1627-40.
3. Xavier, R. J.; Podolsky, D. K., Unravelling the pathogenesis of inflammatory bowel disease. *Nature* **2007**, *448* (7152), 427-434.
4. Mieli-Vergani, G.; Vergani, D.; Czaja, A. J.; Manns, M. P.; Krawitt, E. L.; Vierling, J. M.; Lohse, A. W.; Montano-Loza, A. J., Autoimmune hepatitis. *Nat Rev Dis Primers* **2018**, *4*, 18017.
5. Mackay, I. R., Historical reflections on autoimmune hepatitis. *World J Gastroenterol* **2008**, *14* (21), 3292-300.
6. Wang, Q.; Yang, F.; Miao, Q.; Krawitt, E. L.; Gershwin, M. E.; Ma, X., The clinical phenotypes of autoimmune hepatitis: A comprehensive review. *J Autoimmun* **2016**, *66*, 98-107.
7. Yeoman, A. D.; Longhi, M. S.; Heneghan, M. A., Review article: the modern management of autoimmune hepatitis. *Aliment Pharmacol Ther* **2010**, *31* (8), 771-87.
8. Liberal, R.; Krawitt, E. L.; Vierling, J. M.; Manns, M. P.; Mieli-Vergani, G.; Vergani, D., Cutting edge issues in autoimmune hepatitis. *J Autoimmun* **2016**, *75*, 6-19.
9. Ye, T. H.; Wang, T. T.; Yang, X. X.; Fan, X. L.; Wen, M. Y.; Shen, Y.; Xi, X. T.; Men, R. T.; Yang, L., Comparison of Concanavalin a-Induced Murine Autoimmune Hepatitis Models. *Cell Physiol Biochem* **2018**, *46* (3), 1241-1251.
10. Fukumura, D.; Kashiwagi, S.; Jain, R. K., The role of nitric oxide in tumour progression. *Nat Rev Cancer* **2006**, *6* (7), 521-34.
11. Hofseth, L. J., Nitric oxide as a target of complementary and alternative medicines to prevent and treat inflammation and cancer. *Cancer Lett* **2008**, *268* (1), 10-30.
12. Lundberg, J. O. N.; Lundberg, J. M.; Alving, K.; Weitzberg, E., Nitric oxide and inflammation: The answer is blowing in the wind. *Nature Medicine* **1997**, *3* (1), 30-31.
13. Furchgott, R. F.; Zawadzki, J. V., The obligatory role of endothelial cells in the relaxation of arterial smooth muscle by acetylcholine. *Nature* **1980**, *288* (5789), 373-6.
14. Ignarro, L. J.; Buga, G. M.; Wood, K. S.; Byrns, R. E.; Chaudhuri, G., Endothelium-derived relaxing factor produced and released from artery and vein is nitric oxide. *Proc Natl Acad Sci U S A* **1987**, *84* (24), 9265-9.
15. Gobert, A. P.; Asim, M.; Piazuelo, M. B.; Verriere, T.; Scull, B. P.; de Sablet, T.; Glumac, A.; Lewis, N. D.; Correa, P.; Peek, R. M., Jr.; Chaturvedi, R.; Wilson, K. T., Disruption of nitric oxide signaling by *Helicobacter pylori* results in enhanced inflammation by inhibition of heme oxygenase-1. *J Immunol* **2011**, *187* (10), 5370-9.
16. Bonavida, B.; Garban, H., Nitric oxide-mediated sensitization of resistant tumor cells to apoptosis by chemo-immunotherapeutics. *Redox Biol* **2015**, *6*, 486-94.
17. Crook, K. R.; Jin, M.; Weeks, M. F.; Rampersad, R. R.; Baldi, R. M.; Glekas, A. S.; Shen, Y.; Esserman, D. A.; Little, P.; Schwartz, T. A.; Liu, P., Myeloid-derived suppressor cells regulate T cell and B cell responses during autoimmune disease. *J Leukoc Biol* **2015**, *97* (3), 573-82.
18. Marshall, H. E.; Merchant, K.; Stamler, J. S., Nitrosation and oxidation in the regulation of gene expression. *FASEB J* **2000**, *14* (13), 1889-900.
19. Peng, H. B.; Libby, P.; Liao, J. K., Induction and stabilization of I kappa B alpha by nitric oxide mediates inhibition of NF-kappa B. *J Biol Chem* **1995**, *270* (23), 14214-9.

20. Wallace, J. L.; Ianaro, A.; Flannigan, K. L.; Cirino, G., Gaseous mediators in resolution of inflammation. *Semin Immunol* **2015**, *27* (3), 227-33.
21. Garcia-Ortiz, A.; Serrador, J. M., Nitric Oxide Signaling in T Cell-Mediated Immunity. *Trends Mol Med* **2018**, *24* (4), 412-427.
22. McClure, K. F.; Letavic, M. A.; Kalgutkar, A. S.; Gabel, C. A.; Audoly, L.; Barberia, J. T.; Braganza, J. F.; Carter, D.; Carty, T. J.; Cortina, S. R.; Dombroski, M. A.; Donahue, K. M.; Elliott, N. C.; Gibbons, C. P.; Jordan, C. K.; Kuperman, A. V.; Labasi, J. M.; Laliberte, R. E.; McCoy, J. M.; Naiman, B. M.; Nelson, K. L.; Nguyen, H. T.; Peese, K. M.; Sweeney, F. J.; Taylor, T. J.; Trebino, C. E.; Abramov, Y. A.; Laird, E. R.; Volberg, W. A.; Zhou, J.; Bach, J.; Lombardo, F., Structure-activity relationships of triazolopyridine oxazole p38 inhibitors: identification of candidates for clinical development. *Bioorg Med Chem Lett* **2006**, *16* (16), 4339-44.
23. Nayana, M. R. S.; Sekhar, Y. N.; Kumari, N. S.; Mahmood, S. K.; Ravikumar, M., CoMFA and docking studies on triazolopyridine oxazole derivatives as p38 MAP kinase inhibitors. *European Journal of Medicinal Chemistry* **2008**, *43* (6), 1261-1269.
24. Jerome, K. D.; Rucker, P. V.; Xing, L.; Shieh, H. S.; Baldus, J. E.; Selness, S. R.; Letavic, M. A.; Braganza, J. F.; McClure, K. F., Continued exploration of the triazolopyridine scaffold as a platform for p38 MAP kinase inhibition. *Bioorganic & Medicinal Chemistry Letters* **2010**, *20* (2), 469-473.
25. Kalgutkar, A. S.; Hatch, H. L.; Kosea, F.; Nguyen, H. T.; Choo, E. F.; McClure, K. F.; Taylor, T. J.; Henne, K. R.; Kuperman, A. V.; Dombroski, M. A.; Letavic, M. A., Preclinical pharmacokinetics and metabolism of 6-(4-(2,5-difluorophenyl)oxazol-5-yl)-3-isopropyl-[1,2,4]-triazolo[4,3-a]pyridine, a novel and selective p38 α inhibitor: identification of an active metabolite in preclinical species and human liver microsomes. *Biopharm Drug Dispos* **2006**, *27* (8), 371-86.
26. Zhao, J.; Fang, L.; Zhang, X.; Liang, Y.; Gou, S., Synthesis and biological evaluation of new [1,2,4]triazolo[4,3-a]pyridine derivatives as potential c-Met inhibitors. *Bioorg Med Chem* **2016**, *24* (16), 3483-93.
27. Lu, T.; Alexander, R.; Connors, R. W.; Cummings, M. D.; Galemno, R. A.; Hufnagel, H. R.; Johnson, D. L.; Khalil, E.; Leonard, K. A.; Markotan, T. P., Triazolopyridazines as kinase modulators. Google Patents: 2011.
28. Kim, D.; Wang, L.; Beconi, M.; Eiermann, G. J.; Fisher, M. H.; He, H.; Hickey, G. J.; Kowalchick, J. E.; Leiting, B.; Lyons, K.; Marsilio, F.; McCann, M. E.; Patel, R. A.; Petrov, A.; Scapin, G.; Patel, S. B.; Roy, R. S.; Wu, J. K.; Wyvratt, M. J.; Zhang, B. B.; Zhu, L.; Thornberry, N. A.; Weber, A. E., (2R)-4-oxo-4-[3-(trifluoromethyl)-5,6-dihydro[1,2,4]triazolo[4,3-a]pyrazin-7(8H)-yl]-1-(2,4,5-trifluorophenyl)butan-2-amine: a potent, orally active dipeptidyl peptidase IV inhibitor for the treatment of type 2 diabetes. *Journal of medicinal chemistry* **2005**, *48* (1), 141-51.
29. Chen, Y.; Fu, W. L.; Gan, X. D.; Xing, W. W.; Xia, W. R.; Zou, M. J.; Liu, Q.; Wang, Y. Y.; Zhang, C.; Xu, D. G., SAK-HV Promotes RAW264.7 cells Migration Mediated by MCP-1 via JNK and NF-kappaB Pathways. *Int J Biol Sci* **2018**, *14* (14), 1993-2002.
30. Arana, L.; Ordonez, M.; Ouro, A.; Rivera, I. G.; Gangoiti, P.; Trueba, M.; Gomez-Munoz, A., Ceramide 1-phosphate induces macrophage chemoattractant protein-1 release: involvement in ceramide 1-phosphate-stimulated cell migration. *Am J Physiol Endocrinol Metab* **2013**, *304* (11), E1213-26.
31. Camps, M.; Ruckle, T.; Ji, H.; Ardisson, V.; Rintelen, F.; Shaw, J.; Ferrandi, C.; Chabert, C.; Gillieron, C.; Francon, B.; Martin, T.; Gretener, D.; Perrin, D.; Leroy, D.; Vitte, P. A.; Hirsch, E.; Wymann, M. P.; Cirillo, R.; Schwarz, M. K.; Rommel, C., Blockade of PI3K γ suppresses joint inflammation and damage in mouse models of rheumatoid arthritis. *Nat Med* **2005**, *11* (9), 936-43.
32. Wang, Z. L.; Wu, X. H.; Song, L. F.; Wang, Y. S.; Hu, X. H.; Luo, Y. F.; Chen, Z. Z.; Ke, J.; Peng, X. D.; He, C. M.; Zhang, W.; Chen, L. J.; Wei, Y. Q., Phosphoinositide 3-kinase gamma inhibitor ameliorates concanavalin A-induced hepatic injury in mice. *Biochem Biophys Res Commun* **2009**, *386* (4), 569-74.
33. Tang, M. L.; Zhong, C.; Liu, Z. Y.; Peng, P.; Liu, X. H.; Sun, X., Discovery of novel sesquiterpene indanone analogues as potent anti-inflammatory agents. *European Journal of Medicinal Chemistry* **2016**, *113*, 63-74.
34. Webb, G. J.; Hirschfield, G. M.; Krawitt, E. L.; Gershwin, M. E., Cellular and Molecular Mechanisms of Autoimmune Hepatitis. *Annu Rev Pathol* **2018**, *13*, 247-292.

35. Manns, M. P.; Czaja, A. J.; Gorham, J. D.; Krawitt, E. L.; Mieli-Vergani, G.; Vergani, D.; Vierling, J. M.; American Association for the Study of Liver, D., Diagnosis and management of autoimmune hepatitis. *Hepatology* **2010**, *51* (6), 2193-213.
36. European Association for the Study of the, L., EASL Clinical Practice Guidelines: Autoimmune hepatitis. *J Hepatol* **2015**, *63* (4), 971-1004.
37. Sun, C.; Sher, P. M.; Wu, G.; Ewing, W. R.; Huang, Y.; Lee, T.; Murugesan, N.; Sulsky, R. B. Preparation of triazolopyridine derivatives as cannabinoid receptor 1 antagonists. WO2006138695A1, 2006.
38. Corkey, B.; Elzein, E.; Jiang, R.; Kalla, R.; Kobayashi, T.; Koltun, D.; Li, X.; Notte, G.; Parkhill, E.; Perry, T.; Zablocki, J. Preparation of [1,2,4]triazolo[4,3-a]pyridine derivatives and analogous as sodium channel modulators. US20110021521A1, 2011.
39. Kennedy-Smith, J. J.; Arora, N.; Billedeau, J. R.; Fretland, J.; Hang, J. Q.; Heilek, G. M.; Harris, S. F.; Hirschfeld, D.; Javanbakht, H.; Li, Y.; Liang, W. L.; Roetz, R.; Smith, M.; Su, G. P.; Suh, J. M.; Villasenor, A. G.; Wu, J.; Yasuda, D.; Klumpp, K.; Sweeney, Z. K., Synthesis and biological activity of new pyridone diaryl ether non-nucleoside inhibitors of HIV-1 reverse transcriptase. *Medchemcomm* **2010**, *1* (1), 79-83.
40. Scheufler, C.; Mobitz, H.; Gaul, C.; Ragot, C.; Be, C.; Fernandez, C.; Beyer, K. S.; Tiedt, R.; Stauffer, F., Optimization of a Fragment-Based Screening Hit toward Potent DOT1L Inhibitors Interacting in an Induced Binding Pocket. *ACS Medicinal Chemistry Letters* **2016**, *7* (8), 730-734.
41. Adams, N. D.; Burgess, J. L.; Darcy, M. G.; Knight, S. D.; Newlander, K. A.; Ridgers, L. H.; Schmidt, S. J. Preparation of quinazoline derivatives as PI3 kinase inhibitors. WO2008157191A2, 2008.
42. Xue, J.; Chen, F.; Wang, J.; Wu, S.; Zheng, M.; Zhu, H.; Liu, Y.; He, J.; Chen, Z., Emodin protects against concanavalin A-induced hepatitis in mice through inhibiting activation of the p38 MAPK-NF-kappaB signaling pathway. *Cell Physiol Biochem* **2015**, *35* (4), 1557-70.
43. Ye, T. H.; Yang, F. F.; Zhu, Y. X.; Li, Y. L.; Lei, Q.; Song, X. J.; Xia, Y.; Xiong, Y.; Zhang, L. D.; Wang, N. Y.; Zhao, L. F.; Gou, H. F.; Xie, Y. M.; Yang, S. Y.; Yu, L. T.; Yang, L.; Wei, Y. Q., Inhibition of Stat3 signaling pathway by nifuroxazide improves antitumor immunity and impairs colorectal carcinoma metastasis. *Cell Death Dis* **2017**, *8* (1), e2534.

Highlights

A series of new (1,2,4)triazole[4,3-a]pyridine derivatives were synthesized.

8d suppressed NF- κ B p65 translocation and expression of inflammatory genes.

Preliminary mechanisms of anti-inflammatory action were discovered.

8d could be a lead compound as AIH therapeutic agent.